J Neurophysiol 120: 1712–1727, 2018.
First published July 5, 2018; doi:10.1152/jn.00257.2018.

RESEARCH ARTICLE | *Cellular and Molecular Properties of Neurons*

Electrophysiological properties of medium spiny neurons in the nucleus accumbens core of prepubertal male and female *Drd1a*-tdTomato line 6 BAC transgenic mice

Jinyan Cao,[1,2] David M. Dorris,[1] and John Meitzen[1,2,3,4]

[1]*Department of Biological Sciences, North Carolina State University, Raleigh, North Carolina;* [2]*W. M. Keck Center for Behavioral Biology, North Carolina State University, Raleigh, North Carolina;* [3]*Center for Human Health and the Environment, North Carolina State University, Raleigh, North Carolina; and* [4]*Comparative Medicine Institute, North Carolina State University, Raleigh, North Carolina*

Submitted 20 April 2018; accepted in final form 30 June 2018

Cao J, Dorris DM, Meitzen J. Electrophysiological properties of medium spiny neurons in the nucleus accumbens core of prepubertal male and female *Drd1a*-tdTomato line 6 BAC transgenic mice. *J Neurophysiol* 120: 1712–1727, 2018. First published July 5, 2018; doi:10.1152/jn.00257.2018.—The nucleus accumbens core (AcbC) is a striatal brain region essential for integrating motivated behavior and reward processing with premotor function. In humans and rodents, research has identified sex differences and sex steroid hormone sensitivity in AcbC-mediated behaviors, in disorders, and in rats in the electrophysiological properties of the AcbC output neuron type, the medium spiny neuron (MSN). It is unknown whether the sex differences detected in MSN electrophysiological properties extend to mice. Furthermore, MSNs come in distinct subtypes with subtle differences in electrophysiological properties, and it is unknown whether MSN subtype-specific electrophysiology varies by sex. To address these questions, we used male and female Drd1a-tdTomato line 6 bacterial artificial chromosome transgenic mice. We made acute brain slices of the AcbC, and performed whole cell patch-clamp recordings across MSN subtypes to comprehensively assess AcbC MSN subtype electrophysiological properties. We found that (*1* mice MSNs did not exhibit the sex differences detected in rat MSNs, and *2*) electrophysiological properties differed between MSN subtypes in both sexes, including rheobase, resting membrane potential, action potential properties, intrinsic excitability, input resistance in both the linear and rectified ranges, and miniature excitatory postsynaptic current properties. These findings significantly extend previous studies of MSN subtypes performed in males or animals of undetermined sex and indicate that the influence of sex upon AcbC MSN properties varies between rodent species.

NEW & NOTEWORTHY This research provides the most comprehensive assessment of medium spiny neuron subtype electrophysiological properties to date in a critical brain region, the nucleus accumbens core. It additionally represents the first evaluation of whether mouse medium spiny neuron subtype electrophysiological properties differ by sex.

medium spiny neuron; mice; nucleus accumbens; sex; ventral striatum

INTRODUCTION

The nucleus accumbens core (AcbC) is a striatal brain region critical for integrating limbic and premotor function (Mogenson et al. 1980; Morrison et al. 2017). These functions include regulating motivated, social, and reward-related behaviors, select emotional processes, and disorders such as depression and drug addiction (Salgado and Kaplitt 2015; Yager et al. 2015). All of these behaviors and disorders exhibit sex differences in incidence and/or phenotype, including in many cases sensitivity to sex steroid hormones such as 17β-estradiol (Becker and Koob 2016; Carroll and Anker 2010; McLean and Anderson 2009; Yoest et al. 2018; Young and Korszun 2010). The predominant and output neuron type of the AcbC and other striatal regions is the medium spiny neuron (MSN). MSNs synthesize glutamatergic inputs with dopaminergic, GABAergic, cholinergic, and numerous other inputs to regulate internal AcbC targets and efferent targets outside of the AcbC (Smith et al. 2013; Yager et al. 2015). MSNs come in at least two subtypes, which differ in dopamine receptor complement, neuropeptide expression, and electrophysiological properties (Ade et al. 2011; Cepeda et al. 2008; Chan et al. 2012; Fieblinger et al. 2014; Friend and Kravitz 2014; Gerfen et al. 1990; Gertler et al. 2008; Kramer et al. 2011; Kreitzer and Berke 2011; Ma et al. 2012, 2013; Planert et al. 2013; Schier et al. 2017; Sebel et al. 2017; Shuen et al. 2008). One MSN subtype expresses the gene *drd1a*, which produces dopamine D1 receptors, and manufactures the neuropeptides substance P and dynorphin. The other MSN subtype expresses the gene *drd2*, which produces dopamine D2 receptors, and manufactures the neuropeptide enkephalin. Drd1a and Drd2-positive MSN subtypes play specific roles in nucleus accumbens-mediated behaviors and disorders such as depression and drug addiction (Francis and Lobo 2017; Lobo and Nestler 2011) and generally but not exclusively exhibit distinct efferent targets (Gerfen 1992; Kupchik et al. 2015; Nicola 2007; Smith et al. 2013). Experiments documenting the differential electrophysiological properties between MSN subtypes across the striatum have only been performed in mice or rats of either unreported sex or solely in males, consistent with most other neuroscience preclinical studies (Beery and Zucker 2011; Shansky and Woolley 2016; Will et al. 2017). It is

Address for reprint requests and other correspondence: J. Meitzen, Dept. of Biological Sciences, NC State Univ. Campus Box 7617, 144 David Clark Labs Raleigh, NC 27695-7617 (e-mail: jemeitze@ncsu.edu).

unknown whether subtype-specific differences in MSN electrophysiology are present in both males and females.

This gap in knowledge between male and female MSN subtype physiology is relevant for investigation, both because of the aforementioned sex differences in AcbC function but also because sex differences have been detected in dopaminergic and, more recently documented, glutamatergic synaptic transmission (Becker and Hu 2008; Cao et al. 2016; Di Paolo 1994; Forlano and Woolley 2010; Peterson et al. 2015, 2016; Sazdanovic et al. 2013; Staffend et al. 2011; Wissman et al. 2011, 2012). MSNs receive glutamatergic inputs from multiple neural loci such as but not limited to the prefrontal cortex and hippocampus (Groenewegen et al. 1999; Kelley 2004). Sex differences in glutamatergic synapse properties include increased excitatory synapse number and dendritic spine density in adult female compared with male rat AcbC (Forlano and Woolley 2010; Wissman et al. 2011, 2012). This sex difference manifests in electrophysiological experiments in prepubertal and adult rats as a robust approximately twofold elevation in miniature excitatory postsynaptic current (mEPSC) frequencies onto female compared with male AcbC MSNs (Cao et al. 2016; Wissman et al. 2011). In human postmortem nucleus accumbens, dendritic spine density, a neuroanatomical correlate of excitatory synapse number, is likewise increased in female compared with male MSNs (Sazdanovic et al. 2013). It is unknown whether female mouse mEPSC properties and other excitatory synapse properties are similar to those detected in female rats.

We addressed these questions using male and female B6 *Cg-Tg (Drd1a*-tdTomato) line 6 Calak/J hemizygous mice, which were first developed in the laboratory of Dr. Nicole Calakos (Ade et al. 2011) and build on a number of bacterial artificial chromosome (BAC) transgenic mouse lines that have proven to be useful tools for elucidating the contributions of neuron subtypes (Ting and Feng 2014; Valjent et al. 2009). This particular transgenic mouse line features a highly sensitive and specific fluorescent reporter for Drd1a-expressing MSNs, allowing for accurate differentiation of MSN subtypes within a single mouse. Additional advantages of this specific transgenic mouse line over other relevant lines are that it exhibits normal striatal-mediated behaviors and appears to express no obvious physical or cellular deformities (Ade et al. 2011; Enoksson et al. 2012; Thibault et al. 2013). We made acute brain slices of female and male AcbC and then employed whole-cell patch clamp recording of individual MSN subtypes to perform the most comprehensive analysis of AcbC MSN subtype electrophysiological properties to date. We specifically test the hypotheses that MSN electrophysiological attributes differ by subtype and sex, including individual action potential, excitability, input resistance, passive membrane, and mEPSC properties.

MATERIALS AND METHODS

Animals. Male B6 *Cg-Tg (Drd1a*-tdTomato) line 6 Calak/J mice and female C57BL/6 background mice were purchased from the Jackson Laboratory (JAX stock no. 16204). During the first week after arrival, mice were individually housed. After the first week, mice were housed in male and female pairs to enable breeding of hemizygous offspring. Offspring aged postnatal day (PND) 16–24 from F1 litters were used in experiments. Age was matched between experimental groups (Drd1a-positive male: 19.50 ± 1.80; Drd1a-positive female: 19.47 ± 2.20; Drd2-positive male: 19.61 ± 1.59; and Drd2-positive female: 19.76 ± 2.49). Mice were not weaned before experimental use, and female vaginal opening had not occurred before experimental use. Pups were ear punched for identification and genotyping. Mice were housed in a temperature- and light-controlled room (22 ± 1°C, 40–45% humidity, 12:12-h light-dark cycle, lights on at 7:00 AM) at the Biological Resource Facility of North Carolina State University. All cages were washed polysulfone bisphenol A free and were filled with bedding manufactured from virgin hardwood chips (Beta Chip; NEPCO, Warrensburg, NY) to avoid the endocrine disruptors present in corncob bedding (Mani et al. 2005; Markaverich et al. 2002; Villalon Landeros et al. 2012). Soy protein-free rodent chow (2020X; Teklad) and glass-bottle provided water were available ad libitum. All animals in these studies were maintained according to the applicable portions of the Animal Welfare Act and the U.S. Department of Health and Human Services *Guide for the Care and Use of Laboratory Animals*, and the study was approved by Institutional Animal Care and Use Committee at North Carolina State University.

Animal genotyping. Mice genotyping was performed by Celplor (Raleigh, NC), using the following primers according to the Jackson Laboratory suggested protocol: Transgene Forward [forward primer, (12153), 5-CTT CTG AGG CGG AAA GAA CC-3) and Transgene Reverse [reverse primer (12154), 5-TTT CTG ATT GAG AGC ATT CG-3]; PCR product length is 750 basepairs. The internal control was: Internal Positive Control Forward (oIMR7338), CTA GGC CAC AGA ATT GAA AGA TCT; and Internal Positive Control Reverse (oIMR7339), GTA GGT GGA AAT TCT AGC ATC ATC C); PCR product length is 324 basepairs. PCR was performed according to the suggested protocol from Jackson Laboratory: 1 cycle of 94°C for 2 min, 5 cycles of 94°C for 30 s, 60–55°C touchdown ramp for 30 s and 72°C for 30 s, 25 cycles of 94°C for 30 s, 55°C for 30 s, and 72°C for 30 s, followed by 1 cycle of 72°C for 5 min.

Acute brain slice preparation. Brain slices for electrophysiological recordings were prepared as previously described (Dorris et al. 2014). Briefly, mice were deeply anesthetized with isoflurane gas and killed by decapitation. The brain was then dissected rapidly into ice-cold, oxygenated sucrose artificial cerebellum spinal fluid (s-ACSF) containing the following (in mM): 75 sucrose, 1.25 NaH_2PO_4, 3 $MgCl_2$, 0.5 $CaCl_2$, 2.4 Na pyruvate, and 1.3 ascorbic acid from Sigma-Aldrich (St. Louis, MO) and 75 NaCl, 25 $NaHCO_3$, 15 dextrose, and 2 KCl from Fisher (Pittsburg, PA). The osmolarity of the s-ACSF was between 295 and 305 mosM, and pH was between 7.2 and 7.4. Coronal brain slices (300 μm) were prepared using a vibratome and then incubated in regular ACSF containing the following (in mM): 126 NaCl, 26 $NaHCO_3$, 10 dextrose, 3 KCl, 1.25 NaH_2PO_4, 1 $MgCl_2$, and 2 $CaCl_2$ (295–305 mosM, pH 7.2–7.4) for 30 min at 30 ± 1°C and then at least 30 min at room temperature (21–23°C). Slices were stored submerged in room temperature, oxygenated ACSF for up to 5 h after sectioning in a large volume bath holder.

Electrophysiological recording. Slices were allowed to rest at least 1 h after sectioning and were then placed in a Zeiss Axioscope equipped with IR-DIC and fluorescent optics, a Dage IR-1000 video camera, and ×10 and ×40 lenses with optical zoom. Slices were superfused with oxygenated ACSF heated to ~27°C (Drd1a-positive male: 27.68 ± 0.86°C; Drd2-positive male: 27.35 ± 0.71°C; Drd1a-positive female: 27.63 ± 0.45°C; and Drd2-positive female: 27.47 ± 0.79°C). Whole cell patch-clamp recordings were used to record the electrical properties of fluorescently labeled Drd1a-positive and unlabeled Drd2-positive MSNs in the AcbC (Fig. 1). Only clearly fluorescently labeled and nonlabeled neurons were selected for recording. AcbC gross regional volume and cell density and soma size do not appear to vary by sex in rodents and humans (Meitzen et al. 2011; Wong et al. 2016). Glass electrodes (12–20 MΩ) contained the following solution (in mM): 115 K D-gluconate, 8 NaCl, 2 EGTA, 2 $MgCl_2$, 2 MgATP, 0.3 NaGTP, and10 phosphocreatine from Sigma-Aldrich and 10 HEPES from Fisher (285 mosM, pH 7.2–7.4). Signals were amplified, filtered (2 kHz), and digitized (10 kHz) with a

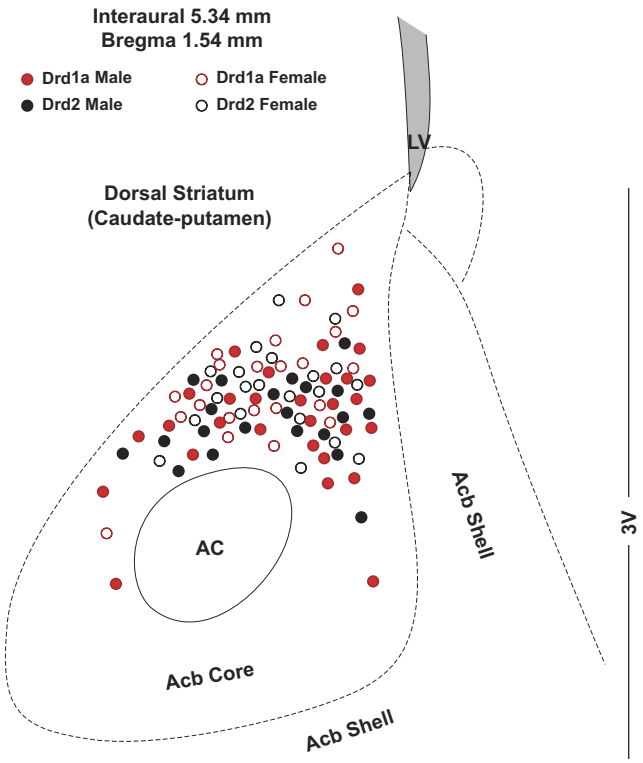

Fig. 1. Location of whole-cell patch clamped medium spiny neurons (MSNs) sorted by subtype in the nucleus accumbens core of female and male Drd1a-tdTomato line 6 BAC transgenic mice. "Drd1a" males and females represent recordings from fluorescently labeled Drd1a-positive MSNs. "Drd2 " males and females represent recordings from nonfluorescently labeled MSNs, which are almost exclusively Drd2-positive MSNs. ACB, nucleus accumbens; AC, anterior commissure; LV, lateral ventricle; 3V, third ventricle.

MultiClamp 700B amplifier attached to a Digidata 1550 system and a personal computer using pClamp 10 software. Membrane potentials were corrected for a calculated liquid junction potential of −13.5 mV. With the use of previously described procedures (Dorris et al. 2015), recordings were first made in current clamp to assess neuronal action potential and passive membrane properties. MSNs were identified by their medium-sized somas, the presence of a slow ramping subthreshold depolarization in response to low-magnitude positive current injections, a hyperpolarized resting membrane potential more negative than −65 mV, an action potential amplitude >25 mV, inward rectification, and prominent spike after hyperpolarization (Belleau and Warren 2000; O'Donnell and Grace 1993).

After MSN identification and current clamp recording, oxygenated ACSF containing both the $GABA_A$ receptor antagonist picrotoxin (PTX; 150 μM; Fisher) and the voltage-gated sodium channel blocker tetrodotoxin (TTX; 1 μm, Abcam Biochemicals) was applied to the bath solution to abolish GABAergic inhibitory postsynaptic current events and action potentials, respectively. Following an established protocol (Cao et al. 2016), once depolarizing current injection no longer generated an action potential after exposure to TTX and PTX, MSNs were voltage clamped at −70 mV and miniature excitatory postsynaptic currents (mEPSCs) were recorded for at least 5 min. In all experiments, input/series resistance was monitored for changes and cells were excluded if resistance changed more than 25%.

Data analysis. Intrinsic electrophysiological properties, action potential, and mEPSC characteristics were recorded and analyzed using pClamp 10. After break-in, the resting membrane potential was first allowed to stabilize ~1–2 min, as in Mu et al. (2010). Then, at least three series of depolarizing and hyperpolarizing current injections were applied to elicit basic neurophysiological properties. The electrophysiological properties measured followed the definitions of Cao et al. (2016), Dorris et al. (2015), Willett et al. (2018), and Willett et al. (2016), which were based on those of Farries et al. (2005), Farries and Perkel (2000, 2002), and Meitzen et al. (2009). For each neuron, measurements were made of at least three action potentials generated from the minimum current injection necessary to elicit one or two action potentials. These measurements were then averaged to generate the reported action potential measurements for that neuron. For action potential measurements, only the first generated action potential was used unless the second action potential was required to meet the standard three action potentials per neuron. Action potential threshold was defined as the first point of sustained positive acceleration of voltage ($\delta^2V/\delta t^2$) that was also more than three times the SD of membrane noise before the detected threshold (Baufreton et al. 2005). The slope of the linear range of the evoked firing rate to positive current curve (FI slope) was calculated from the first current stimulus, which evoked an action potential to the first current stimulus that generated an evoked firing rate that persisted for at least two consecutive current stimuli. Maximum action potential firing rate was assessed in response to +0.10-nA depolarizing injected current. Delay to first action potential was calculated from the minimum current injection necessary to elicit initial action potential production. Input resistance in the linear, nonrectified range was calculated from the steady-state membrane potential in response to −0.02-nA hyperpolarizing injected current. Rectified range input resistance, inward rectification, and percent inward rectification (RRIR/IR × 100) was calculated using the most hyperpolarizing current injected into the MSN, as in Belleau and Warren (2000). The membrane time constant was calculated by fitting a single exponential curve to the membrane potential change in response to −0.02-nA hyperpolarizing pulses. The sag index was used to assess possible MSN subtype and sex differences in hyperpolarization-induced "sag" (i.e., I_h current) (Farries et al. 2005). The sag index is the difference between the minimum voltage measured during the largest hyperpolarizing current pulse and the steady-state voltage deflection of that pulse, divided by the steady-state voltage deflection. mEPSCs frequency, amplitude, and decay were analyzed offline using Mini Analysis (Synaptosoft, http://www.synaptosoft.com/MiniAnalysis/). Threshold was set as 5 pA, noise filter was set at 1,000 Hz, and accurate event detection was validated by visual inspection.

Statistics. Experiments were analyzed via a two-way ANOVA with either a Sidak or Newman-Keuls multiple comparisons post hoc test, as appropriate (Excel version 2010, Microsoft, Redmond, WA; Prism version 6.07, GraphPad Software, La Jolla, CA). $P < 0.05$ was considered a priori as significant. Effect size was assessed using Cohen's d value. d Values are reported numerically and were classified a priori as small (>0.20), medium (>0.50), and large (>0.80) (Cohen 1977). Data are presented as means ± SE.

RESULTS

We recorded a total of 93 MSNs from the AcbC of male and female B6 *Cg-Tg (Drd1a*-tdTomato) 6 Calak/J hemizygous mice. Recorded MSNs were divided into four experimental groups: male tdTomato-labeled Drd1a-positive MSNs, female tdTomato-labeled Drd1a-positive MSNs, male tdTomato-unlabeled MSNs, and female tdTomato-unlabeled MSNs. Unlabeled MSNs almost exclusively comprise the Drd2-positive MSN subtype, including during the developmental age and striatal region assessed in this study (Ade et al. 2011; Enoksson et al. 2012; Thibault et al. 2013). In this mouse line tdTomato-unlabled MSNs have a very low (~1.6%) contamination with Drd1a-positive MSNs. Thus, in this study, we refer to all tdTomato-unlabeled MSNs as Drd2-positive MSNs, with the acknowledgment that this designation is putative.

Table 1. *Action potential properties of Drd1a- and Drd2-positive mouse medium spiny neurons*

MSN Subtype	AP Threshold, mV	AP Width, ms	AHP Peak, mV	AHP Time to Peak, ms	Rheobase, nA	FI Slope, Hz/nA	Delay to first AP, ms	Maximum firing rate (Hz)
Drd1a male (28)	-51.43 ± 5.78^{a}	2.31 ± 0.41^{a}	-8.25 ± 3.47^{a}	35.91 ± 11.58^{a}	0.07 ± 0.03^{a}	256.65 ± 72.50^{a}	517.3 ± 30.1^{a}	13.39 ± 1.67^{a}
Drd2 male (21)	-53.73 ± 3.67^{a}	$2.82 \pm 0.61^{b,c}$	$-5.32 \pm 2.17^{b,c}$	$26.94 \pm 12.50^{b,c}$	0.04 ± 0.02^{b}	347.70 ± 117.78^{b}	311.8 ± 24.23^{b}	24.04 ± 2.46^{b}
Drd1a female (23)	-51.26 ± 4.16^{a}	$2.50 \pm 0.35^{a,b,c}$	$-7.05 \pm 2.76^{a,b,c}$	$30.85 \pm 8.55^{a,b,c}$	0.07 ± 0.03^{a}	260.80 ± 88.38^{a}	488.5 ± 33.57^{a}	$16.37 \pm 2.36^{a,c}$
Drd2 female (21)	-52.83 ± 5.36^{a}	$2.79 \pm 0.57^{b,c}$	$-5.82 \pm 2.31^{b,c}$	$26.34 \pm 12.35^{b,c}$	0.05 ± 0.03^{b}	$300.72 \pm 112.60^{a,b}$	321.7 ± 20.86^{b}	$20.98 \pm 1.69^{b,c}$

Values are means ± SE. Numbers in parentheses indicate experimental "*n*." MSN, medium spiny neuron; AP, action potential; AHP, afterhyperpolarization; FI, frequency of evoked spikes to injected depolarization current. [a,b,c]Different superscript letters denote significant differences between groups within a column.

Rheobase, resting membrane potential, and action potential threshold. To test the hypothesis that the electrophysiological properties of MSNs this mouse line differed by subtype and animal sex, we injected MSNs with a series of positive and negative currents and assessed a comprehensive battery of electrophysiological properties (Tables 1 and 2; Fig. 2*A*). Multiple electrophysiological properties varied by subtype, including resting membrane potential and rheobase, the minimum necessary current to trigger action potential generation. The resting membrane potential of Drd1a-positive MSNs was hyperpolarized compared with Drd2-positive MSNs, and overall this did not differ by sex [Fig. 2*B*, *left*, absolute values: subtype: $F_{(1,89)} = 12.05$, $P \leq 0.0008$; sex: $F_{(1,89)} = 1.25$, $P = 0.2669$; interaction: $F_{(1,89)} = 0.14$, $P = 0.9063$] [Fig. 2*B*, *right*, normalized values: subtype: $F_{(1,89)} = 16.20$, $P \leq 0.0001$; sex: $F_{(1,89)} = 0.03$, $P = 0.8656$; interaction: $F_{(1,89)} = 0.03$, $P = 0.8656$]. Compared between groups, the resting membrane potential of male Drd1a-positive MSNs differed from male and female Drd2-positive MSNs ($P < 0.05$, $d = 0.76$; $P < 0.01$, $d = 0.89$, respectively). The resting membrane potential of female Drd1a-positive MSNs only differed from female Drd2-positive MSNs ($P < 0.05$, $d = 0.68$). The rheobase of Drd1a-positive MSNs was increased compared with Drd2-positive MSNs, and overall this did not differ by sex [Fig. 2*C*, *left*, absolute values: subtype: $F_{(1,89)} = 19.04$, $P \leq 0.0001$; sex: $F_{(1,89)} = 0.00$, $P = 0.9995$; interaction: $F_{(1,89)} = 1.34$, $P = 0.2499$] [*Fig*. 2*C*, *right*, normalized values: subtype: $F_{(1,89)} = 19.77$, $P \leq 0.0001$; sex: $F_{(1,89)} = 5.09$, $P = 0.9506$; interaction: $F_{(1,89)} = 1.50$, $P = 0.2237$]. Compared between groups, the rheobase of male Drd1a-positive MSNs differed from male and female Drd2-positive MSNs ($P < 0.001$, $d = 1.17$; $P < 0.01$, $d = 0.87$, respectively), as did female Drd1a-positive MSNs ($P < 0.01$, $d = 1.00$; $P < 0.05$, $d = 0.68$, respectively). No robust differences between subtypes or sex were detected in action potential threshold [Fig. 2*D*, *left*, absolute values: subtype: $F_{(1,89)} = 3.58$, $P = 0.06$; sex: $F_{(1,89)} = 0.28$, $P = 0.6001$; interaction: $F_{(1,89)} = 0.13$, $P = 0.7203$] [Fig. 2*D*, *right*, normalized values: subtype: $F_{(1,89)} = 3.58$, $P = 0.0618$; sex: $F_{(1,89)} = 0.28$, $P = 0.6001$; interaction: $F_{(1,89)} = 0.13$, $P = 0.7203$]. Collectively these data indicate that Drd1a-positive MSNs in both males and females exhibit decreased resting membrane potential and increased rheobase compared with Drd2-positive MSNs, with comparable effect sizes. This difference in rheobase between MSN subtypes seems primarily driven by the difference in resting membrane potential.

Action potential properties. Several action potential properties also varied by MSN subtype, including action potential width, the magnitude of the action potential afterhyperpolarization (AHP) peak, and the action potential AHP time to peak magnitude (Fig. 3*A*). The action potential width of Drd1a-positive MSNs was shorter compared with Drd2-positive MSNs, and the effect size between subtypes was larger in male compared with female MSNs [Fig. 3*B*, *left*, absolute values: subtype: $F_{(1,89)} = 15.44$, $P = 0.0002$; sex: $F_{(1,89)} = 0.15$, $P = 0.4270$; interaction: $F_{(1,89)} = 1.22$, $P = 0.2733$] [Fig. 3*B*, *right*, normalized values: subtype: $F_{(1,89)} = 15.44$, $P = 0.0002$; sex: $F_{(1,89)} = 0.64$, $P = 0.4270$; interaction: $F_{(1,89)} = 1.22$, $P = 0.2733$]. Compared between groups, the action potential width of male Drd1a-positive MSNs differed from male and female Drd2-positive MSNs ($P < 0.01$, $d = 0.51$; $P < 0.01$, $d = 0.97$, respectively), but the action potential width of female Drd1a-positive MSNs did not differ from female Drd2-positive MSNs

Table 2. *Passive properties of Drd1a- and Drd2-positive mouse medium spiny neurons*

Property	Male	Female
Resting membrane potential, mV	Drd1a: -86.98 ± 5.50^{a}	Drd1a: -85.57 ± 5.97^{a}
	Drd2: -82.25 ± 6.92^{b}	Drd2: -80.51 ± 8.67^{b}
Time constant of the membrane, ms	Drd1a: 17.66 ± 8.15^{a}	Drd1a: $20.70 \pm 5.42^{a,b}$
	Drd2: 24.13 ± 10.66^{b}	Drd2: $22.92 \pm 8.53^{a,b}$
Input resistance in the linear range, MΩ	Drd1a: 287.16 ± 100.47^{a}	Drd1a: $323.89 \pm 104.15^{a,b,c}$
	Drd2: 412.11 ± 177.82^{b}	Drd2: $380.62 \pm 129.33^{b,c}$
Input resistance in the rectified range, MΩ	Drd1a: 195.18 ± 57.98^{a}	Drd1a: $217.07 \pm 63.00^{a,b,c}$
	Drd2: 245.84 ± 71.74^{b}	Drd2: $244.16 \pm 53.89^{b,c}$
Inward rectification, MΩ	Drd1a: 91.97 ± 53.66^{a}	Drd1a: $106.82 \pm 50.52^{a,b,c}$
	Drd2: 166.27 ± 116.27^{b}	Drd2: $136.46 \pm 92.54^{b,c}$
% Inward rectification, %	Drd1a: 69.67 ± 8.97^{a}	Drd1a: $68.10 \pm 7.49^{a,b,c}$
	Drd2: 62.58 ± 10.73^{b}	Drd2: $67.55 \pm 14.29^{b,c}$
Sag index	Drd1a: 0.0082 ± 0.0073^{a}	Drd1a: 0.0067 ± 0.007^{9a}
	Drd2: 0.0076 ± 0.0088^{a}	Drd2: 0.0068 ± 0.0067^{a}

Values are means ± SE. Numbers in parentheses indicate experimental "*n*." Different superscript letters denote significant differences between groups within a column. For example, groups sharing the same superscript letter do not statistically differ from each other. Sag index is unitless. None of these neurons exhibited spontaneous action potential generation. MSN, medium spiny neuron.

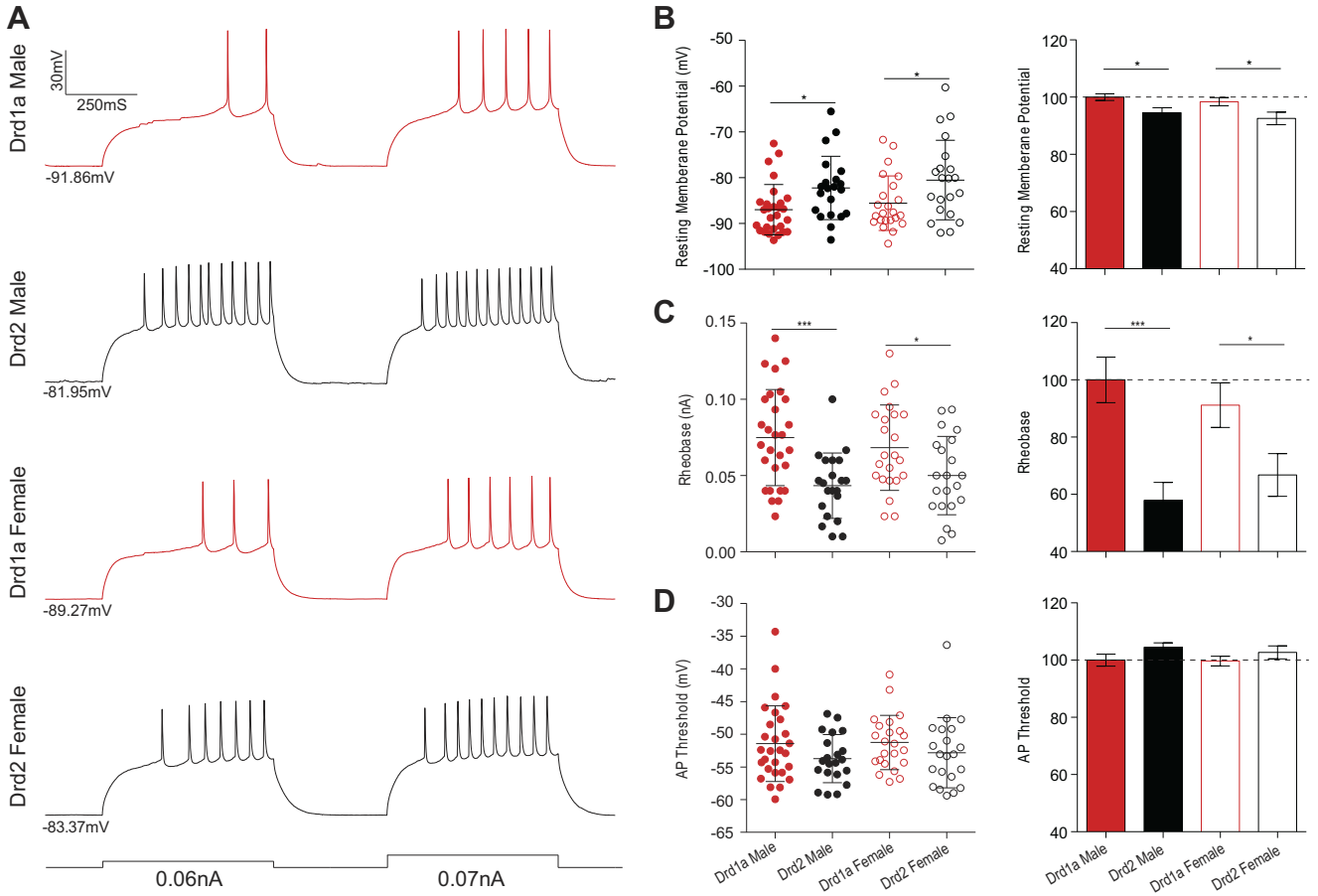

Fig. 2. Resting membrane potential and action potential (AP) rheobase varies by medium spiny neuron (MSN) subtype but not sex. *A*: voltage response of male and female Drd1a-positive and Drd2-positive MSN subtypes to a series of depolarizing current injections. *B*: resting membrane potential is hyperpolarized in male and female Drd1a-positive MSNs compared with Drd2-positive MSNs. *Left*: absolute values. Means ± SE are depicted over individual data points. *Right*: values normalized to male Drd1a-positive MSNs. *C*: rheobase is increased in male and female Drd1a-positive MSNs compared with Drd2-positive MSNs. *Left*: absolute values. *Right*: normalized values. *D*: AP (AP) threshold does not differ between male and female Drd1a-positive MSNs compared with Drd2-positive MSNs. *Left*: absolute values. *Right*: normalized values. $*P < 0.05$; $***P < 0.001$.

($P > 0.05$, $d = 0.05$) or any other group ($P > 0.05$ for all). The magnitude of the action potential AHP peak was larger in Drd1a-positive compared with Drd2-positive MSNs [Fig. 3*C*, *left*, absolute values: subtype: $F_{(1,89)} = 12.78$, $P = 0.0006$; sex: $F_{(1,89)} = 0.36$, $P = 0.5508$; interaction: $F_{(1,89)} = 2.12$, $P = 0.1478$] [Fig. 3*C*, *right*, normalized values: subtype: $F_{(1,89)} = 12.78$, $P = 0.0006$; sex: $F_{(1,89)} = 0.35$, $P = 0.5508$; interaction: $F_{(1,89)} = 2.13$, $P = 0.1478$]. Compared between groups, the magnitude of the action potential AHP peak of male Drd1a-positive MSNs differed from male ($P < 0.01$; $d = 1.01$) and female Drd2-positive MSNs ($P < 0.01$; $d = 0.84$), but the action potential width of female Drd1a-positive MSNs did not differ from any other group, including to female Drd2-positive MSN ($P > 0.05$. $d = 0.48$). Similarly, the action potential AHP time to peak magnitude of Drd1a-positive MSNs was slower compared with Drd2-positive MSNs [Fig. 3*D*, *left*, absolute values: subtype: $F_{(1,89)} = 8.12$, $P = 0.0054$; sex: $F_{(1,89)} = 1.44$, $P = 0.2339$; interaction: $F_{(1,89)} = 0.8935$, $P = 0.3471$] [Fig. 3*D*, *right*, normalized values: subtype: $F_{(1,89)} = 8.12$, $P = 0.0054$; sex: $F_{(1,89)} = 1.43$, $P = 0.2339$; interaction: $F_{(1,89)} = 0.89$, $P = 0.3471$]. Within groups, the action potential AHP time to peak magnitude of male Drd1a-positive MSNs differed from male ($P < 0.05$, $d = 0.74$) and female ($P < 0.05$, $d = 0.80$) Drd2-positive MSNs, but the action potential AHP time to peak magnitude of female Drd1a-positive MSNs did not differ from any other group, including to female Drd2-positive MSN ($P > 0.05$. $d = 0.42$). These differences in action potential properties indicate that Drd1a-positive MSNs exhibit a shorter duration action potential and a more prominent action potential AHP than do Drd2-positive MSNs but that Male MSNs exhibit a larger effect size between subtypes than do female MSNs.

Intrinsic excitability and action potential generation rates. These differences in individual action potential, resting membrane potential, and rheobase properties between MSN subtypes suggest that MSN excitability may also differ. We began our assessment of excitability by analyzing the frequency of action potentials evoked by depolarizing current injections. Action potential firing rates evoked by depolarizing current injections were visibly decreased in male and female Drd1a-positive compared with Drd2-positive MSNs (Fig. 4*A*). This subtype-specific difference in evoked action potential firing rate was more robust in male MSNs than in female MSNs. In male MSNs, Drd1a-positive MSNs exhibited significantly decreased action potential firing rates compared with Drd2-positive MSNs from +0.04- to +0.10-nA injected currents and demonstrated a strong interaction between subtype and injected current [subtype: $F_{(1,1)} = 173.1$, $P < 0.0001$; current: $F_{(1,10)} =$

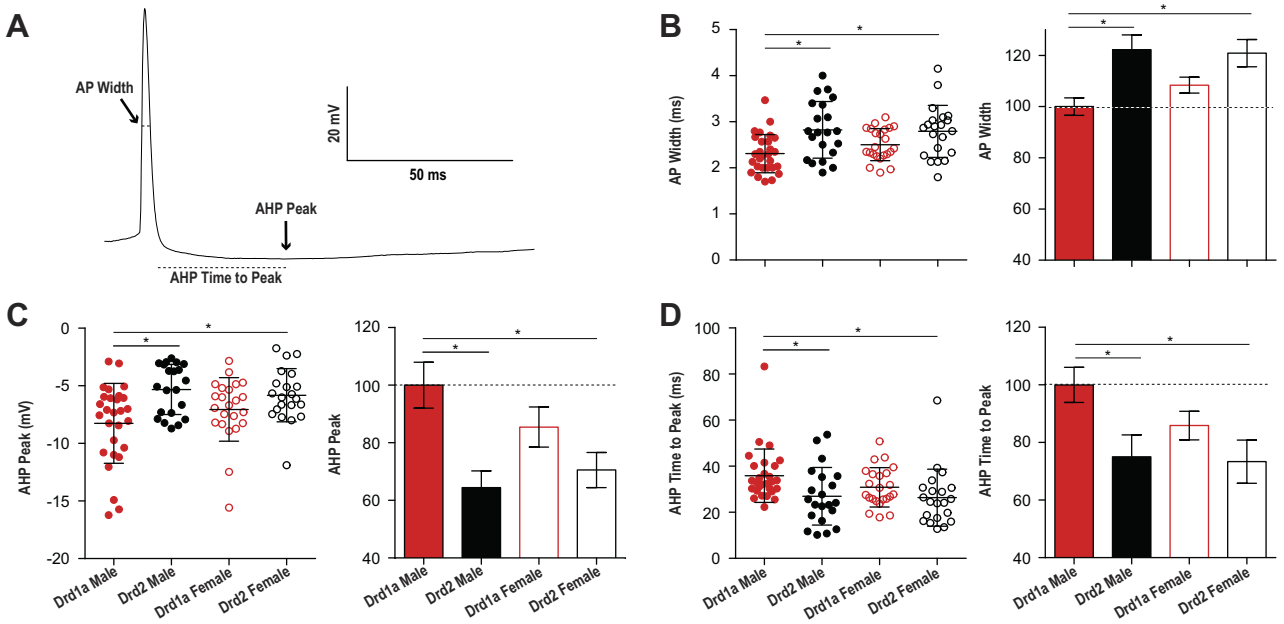

Fig. 3. Action potential (AP) width and afterhyperpolarization (AHP) properties vary by medium spiny neuron (MSN) subtype, with males exhibiting increased MSN subtype differences compared with females. *A*: example individual AP evoked by depolarizing current injection, indicating AP width, AP AHP peak amplitude, and AP AHP time to peak amplitude metrics. *B*: AP width is shorter in Drd1a-positive MSNs compared with Drd2-positive MSNs, with male MSNs exhibiting a larger difference between MSN subtypes than female MSNs. *Left*: absolute values. Means ± SE are depicted over individual data points. *Right*: Values normalized to male Drd1a-positive MSNs. *C*: AP AHP peak amplitude is larger in Drd1a-positive MSNs compared with Drd2-positive MSNs, with male MSNs exhibiting a larger difference between MSN subtypes than female MSNs. *Left*: absolute values. *Right*: normalized values. *D*: AP AHP time to peak amplitude is increased in Drd1a-positive MSNs compared with Drd2-positive MSNs, with male MSNs exhibiting a larger difference between MSN subtypes than female MSNs. *Left*: absolute values. *Right*: normalized values. $*P < 0.05$.

47.84, $P < 0.0001$; interaction: $F_{(1,10)} = 7.248$, $P < 0.0001$; post hoc comparisons: +0.01 to +0.03: $P > 0.05$; +0.04 nA: $P < 0.01$, $d = 0.95$; +0.05 to +0.10 nA: $P < 0.0001$, $d > 1.16$ for all]. In contrast, female Drd1a-positive MSNs exhibited significantly decreased action potential firing rates compared with Drd2-positive MSNs only at the +0.09-nA injected current point and did not demonstrate a significant interaction between subtype and injected current [subtype: $F_{(1,1)} = 34.03$, $P < 0.0001$; current: $F_{(1,10)} = 31.68$, $P < 0.0001$; interaction: $F_{(1,10)} = 1.266$, $P = 0.2474$; post hoc comparisons: +0.09 nA: $P < 0.05$, $d = 0.70$; +0.01 to +0.08, +0.10: $P > 0.05$, $d < 0.69$ for all].

To further probe the relationship among MSN subtype, sex, and neuron excitability, we then quantified the slope of the evoked firing rate to positive current curve (FI slope), the delay to first action potential, and the maximum action potential firing rate generated in response to +0.1-nA current injection. The FI slope of Drd1a-positive MSNs was decreased compared with Drd2-positive MSNs [Fig. 4*B*, *left*, absolute values: subtype: $F_{(1,89)} = 10.36$ $P = 0.0018$; sex: $F_{(1,89)} = 1.11$, $P = 0.2957$; interaction: $F_{(1,89)} = 1.583$, $P = 0.2116$] [Fig. 4*B*, *right*, normalized values: subtype: $F_{(1,89)} = 10.36$ $P = 0.0018$; sex: $F_{(1,89)} = 1.11$, $P = 0.2954$; interaction: $F_{(1,89)} = 1.58$, $P = 0.2122$]. Compared between groups, the FI slope of male Drd1a-positive MSNs differed from male but not female Drd2-positive MSNs ($P < 0.01$, $d = 0.93$; $P > 0.05$, $d = 0.47$, respectively), but the FI slope of female Drd1a-positive MSNs differed from male Drd2-positive MSNs ($P < 0.05$, $d = 0.83$) but not to female Drd2-positive MSNs ($P > 0.05$, $d = 0.39$) or any other group. The delay to first action potential also differed by MSN subtype. The time of this delay reflects the magnitude of the slowly inactivating A-current responsible for the slow ramping subthreshold depolarization found in MSNs (Nisenbaum et al. 1994), and influences evoked action potential generation rates at lower magnitude depolarizing current injections. The delay to first action potential of Drd1a-positive MSNs was increased compared with Drd2-positive MSNs [Fig. 4*C*, *left*, absolute values: subtype: $F_{(1,89)} = 13.77$ $P = 0.0004$; sex: $F_{(1,89)} = 0.00$, $P = 0.9845$; interaction: $F_{(1,89)} = 2.157$, $P = 0.1465$] [Fig. 4*C*, *right*, normalized values: subtype: $F_{(1,89)} = 42.00$ $P < 0.0001$; sex: $F_{(1,89)} = 0.11$, $P = 0.7438$; interaction: $F_{(1,89)} = 0.45$, $P = 0.5033$]. Compared between groups, the delay to first action potential of male Drd1a-positive MSNs differed from male and female Drd2-positive MSNs ($P < 0.0001$, $d > 1.48$ for both), and the delay to first action potential of female Drd1a-positive MSNs differed from male Drd2-positive MSNs ($P < 0.001$, $d = 1.28$) but to no other group, including female Drd2-positive MSNs ($P > 0.05$, $d = 1.26$). The maximum firing rate in response to +0.1-nA current injection also differed between MSN subtypes. The maximum firing rate of Drd1a-positive MSNs was decreased compared with Drd2-positive MSNs, with male MSNs again exhibiting a larger dichotomy than female MSNs [Fig. 4*D*, *left*, absolute values: subtype: $F_{(1,89)} = 42.16$, $P < 0.0001$; sex: $F_{(1,89)} = 0.10$, $P = 0.7535$; interaction: $F_{(1,89)} = 0.47$, $P = 0.4936$] [Fig. 4*D*, *right*, normalized values: subtype: $F_{(1,89)} = 17.76$ $P < 0.0001$; sex: $F_{(1,89)} = 0.00$, $P = 0.9818$; interaction: $F_{(1,89)} = 2.78$, $P = 0.0992$]. Compared between groups, the maximum firing rate of male Drd1a-positive MSNs differed from male and female Drd2-positive MSNs ($P < 0.01$, $d = 1.22$; $P < 0.05$, $d = 1.00$ respectively), and the maximum firing rate of female Drd1a-positive MSNs differed from male Drd2-positive MSNs ($P < 0.05$, $d = 0.80$) but to no other group, including female Drd2-positive MSNs ($P > 0.05$,

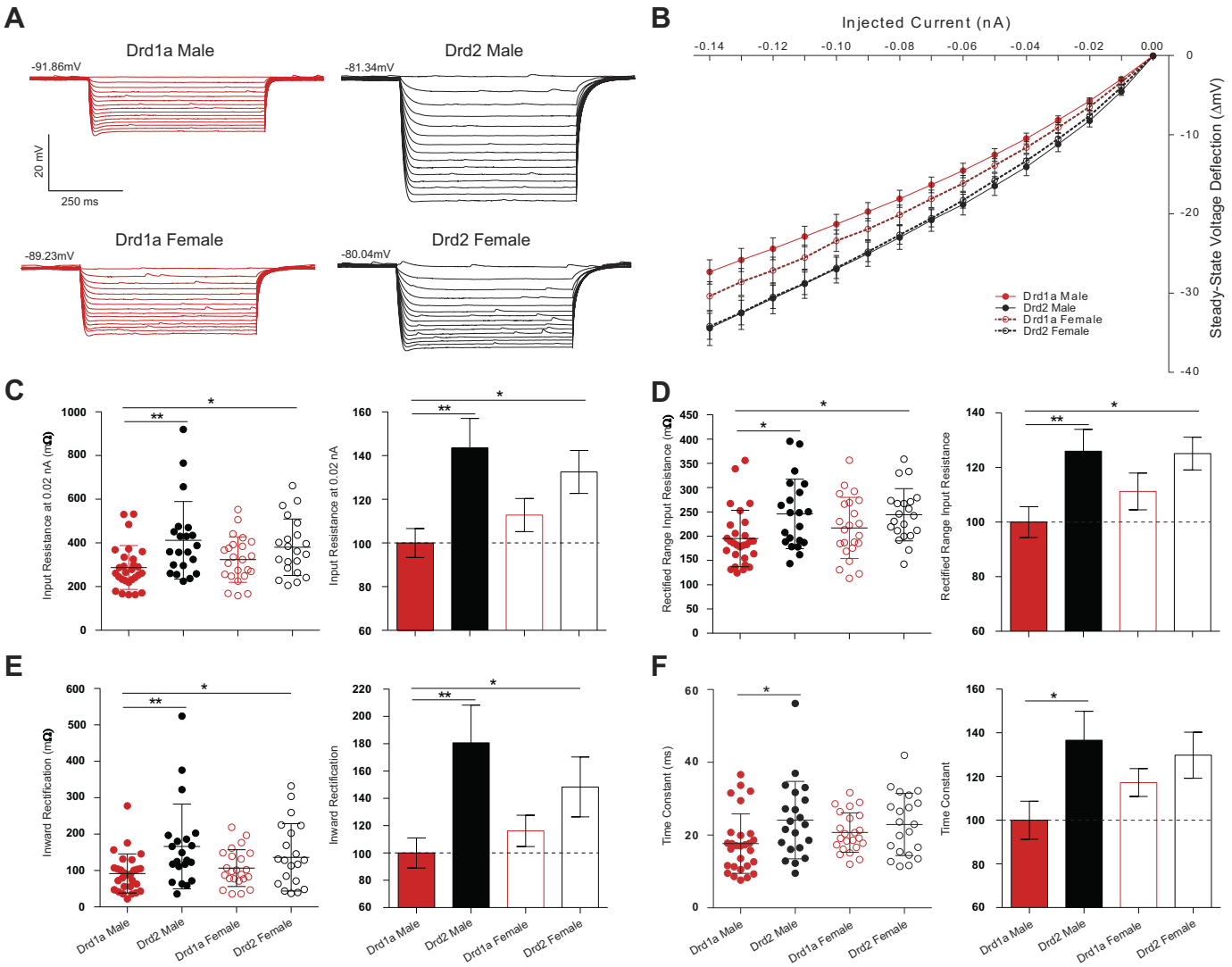

Fig. 5. Input resistance in the rectified and nonrectified ranges by medium spiny neuron (MSN) subtype, with males generally exhibiting increased MSN subtype differences compared with females. *A*: voltage response of male and female Drd1a-positive and Drd2-positive MSN subtypes to a series of negative current injections. *B*: injected negative current to steady-stage voltage deflection curve (*I–V* curve). Red solid circles with red line: Drd1a-positive males; black solid circles with black line: Drd2-positive males; red open circles with dashed red line: Drd1a-positive females; black open circles with dashed black line: Drd2-positive females. *C*: input resistance in the nonrectified range is decreased in Drd1a-positive MSNs compared with Drd2-positive MSNs, with male MSNs exhibiting a larger difference between MSN subtypes than female MSNs. *Left*: absolute values. Means ± SE are depicted over individual data points. *Right*: values normalized to male Drd1a-positive MSNs. *D*: input resistance in the rectified range is decreased in Drd1a-positive MSNs compared with Drd2-positive MSNs, with male MSNs exhibiting a larger difference between MSN subtypes than female MSNs. *Left*: absolute values. *Right*: normalized values. *E*: inward rectification is decreased in Drd1a-positive MSNs compared with Drd2-positive MSNs, with male MSNs exhibiting a larger difference between MSN subtypes than female MSNs. *Left*: absolute values. *Right*: normalized values. *F*: the time constant of the membrane is shorter in Drd1a-positive MSNs compared with Drd2-positive MSNs, with male MSNs exhibiting a larger difference between MSN subtypes than female MSNs. *Left*: absolute values. *Right*: normalized values. $*P < 0.05$; $**P < 0.01$.

$d = 0.53$). This analysis of evoked action potential firing rate (FI slope) maximum firing rate, and the delay to first action potential indicate that Drd1a-positive MSN are much less excitable than Drd2-positive MSNs and that male MSNs exhibit a larger effect size between subtypes than do female MSNs.

Passive membrane properties. We then tested the hypothesis that MSN passive electrophysiological properties differed by subtype and sex, including input resistance in the linear and rectified ranges (Fig. 5*A*), and the time constant of the membrane (Table 2). Overall, MSN passive properties exhibited differences between subtypes that were more robust in male than in female MSNs, including input resistance (Fig. 5*B*). For example, input resistance measured at −0.02-nA current injection in the linear, nonrectified range of Drd1a-positive MSNs was decreased compared with Drd2-positive MSNs, with male MSNs again exhibiting a larger dichotomy than female MSNs [Fig. 5*C*, *left*, absolute values: subtype: $F_{(1,89)} = 11.39$, $P = 0.0011$; sex: $F_{(1,89)} = 0.01$, $P = 0.9225$; interaction: $F_{(1,89)} = 1.61$, $P = 0.2083$] [Fig. 5*C*, *right*, normalized values: subtype: $F_{(1,89)} = 11.39$ $P = 0.0011$; sex: $F_{(1,89)} = 0.01$, $P = 0.9225$; interaction: $F_{(1,89)} = 1.61$, $P = 0.2083$]. Compared between groups, the input resistance in the linear range of male Drd1a-positive MSNs differed from male and female Drd2-positive MSNs ($P < 0.01$, $d = 0.87$; $P < 0.05$, $d = 0.81$, respectively), but the input resistance in the linear range of female Drd1a-

positive MSNs did not differ from any other group, including to female Drd2-positive MSNs ($P > 0.05$, $d = 0.48$). MSNs exhibit substantial inward rectification in response to hyperpolarizing current stimuli (Belleau and Warren 2000; Mermelstein et al. 1998). Input resistance in the rectified range of Drd1a-positive MSNs was decreased compared with Drd2-positive MSNs, with male MSNs again exhibiting a larger dichotomy than female MSNs [Fig. 5*D*, *left*, absolute values: subtype: $F_{(1,89)} = 9.53$, $P = 0.0027$; sex: $F_{(1,89)} = 0.64$, $P = 0.4243$; interaction: $F_{(1,89)} = 0.87$, $P = 0.3520$] [Fig. 5*D*, *right*, normalized values: subtype: $F_{(1,89)} = 9.53$, $P = 0.0027$; sex: $F_{(1,89)} = 0.64$, $P = 0.4243$; interaction: $F_{(1,89)} = 0.87$, $P = 0.3521$]. Compared between groups, the input resistance in the rectified range of male Drd1a-positive MSNs differed from male and female Drd2-positive MSNs ($P < 0.05$, $d = 0.78$; $P < 0.05$, $d = 0.73$, respectively), but the input resistance in the nonrectified range of female Drd1a-positive MSNs did not differ from any group, including to female Drd2-positive MSNs ($P > 0.05$, $d = 0.46$). We then examined inward rectification more extensively by calculating inward rectification (Fig. 5*E*) and percent inward rectification (Table 2). Inward rectification was decreased in Drd1a-positive MSNs compared with Drd2-positive MSNs, with male MSNs again exhibiting a larger effect size between subtypes than female MSNs [Fig. 5*E*, *left*, absolute values: subtype: $F_{(1,89)} = 9.31$, $P = 0.0024$; sex: $F_{(1,89)} = 0.20$, $P = 0.6540$; interaction: $F_{(1,89)} = 1.80$, $P = 0.1827$] [Fig. 5*E*, *right*, normalized values: subtype: $F_{(1,89)} = 9.31$, $P = 0.0024$; sex: $F_{(1,89)} = 0.20$, $P = 0.6540$; interaction: $F_{(1,89)} = 1.80$, $P = 0.1827$]. Compared between groups, the inward rectification of male Drd1a-positive MSNs differed from male and female Drd2-positive MSNs ($P < 0.01$, $d = 0.82$; $P < 0.05$, $d = 0.59$ respectively), but the inward rectification of female Drd1a-positive MSNs did not differ from any group, including female Drd2-positive MSNs ($P > 0.05$, $d = 0.40$). Percent inward rectification exhibited a similar pattern, being increased in Drd1a-positive MSNs compared with Drd2-positive MSNs (Table 2). Along with these measures of inward rectification, the time constant of the membrane also differed between MSN subtypes. The time constant of the membrane was decreased in Drd1a-positive MSNs compared with Drd2-positive MSNs, with male MSNs again exhibiting a larger effect size between subtypes than female MSNs [Fig. 5*F*, *left*, absolute values: subtype: $F_{(1,89)} = 6.46$, $P = 0.0127$; sex: $F_{(1,89)} = 0.29$, $P = 0.5939$; interaction: $F_{(1,89)} = 1.55$, $P = 0.2161$] [Fig. 5*F*, *right*, normalized values: subtype: $F_{(1,89)} = 6.37$, $P = 0.0127$; sex: $F_{(1,89)} = 0.29$, $P = 0.5939$; interaction: $F_{(1,89)} = 1.55$, $P = 0.2161$]. Compared between groups, the time constant of the membrane of male Drd1a-positive MSNs differed from male Drd2-positive MSNs ($P < 0.05$, $d = 0.68$), but the time constant of the membrane of

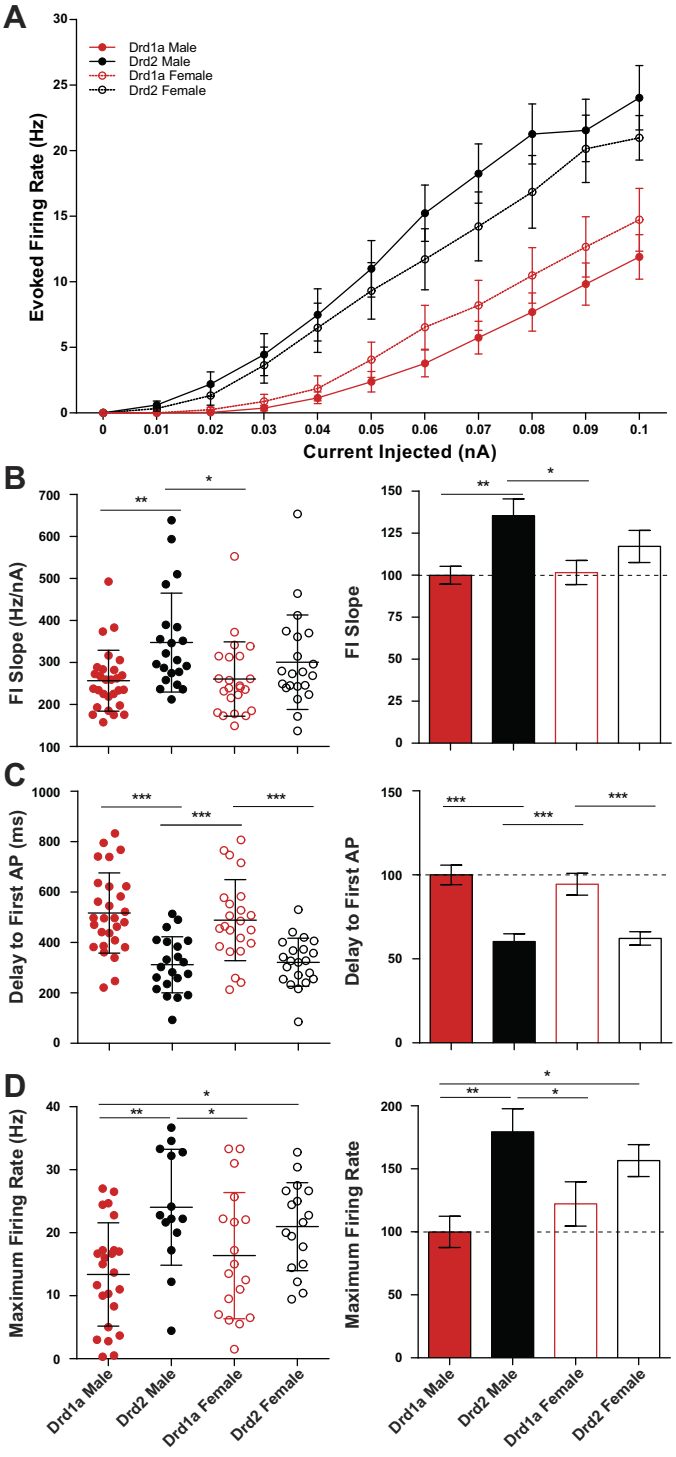

Fig. 4. Action potential (AP) firing rates evoked by depolarizing current injections vary by medium spiny neuron (MSN) subtype, with males exhibiting increased MSN subtype differences compared with females. *A*: AP firing rate evoked by depolarizing current injection was decreased in Drd1a-positive MSNs compared with Drd2-positive MSNs, with male MSNs exhibiting a larger difference between MSN subtypes than female MSNs. In male MSNs, Drd1a-positive MSNs exhibited significantly decreased AP firing rates compared with Drd2-positive MSNs from +0.04- to +0.10-nA injected currents and demonstrated a strong interaction between subtype and injected current. In female MSNs, Drd1a-positive MSNs exhibited significantly decreased AP firing rates compared with Drd2-positive MSNs only at the +0.09-nA injected current point and did not demonstrate a significant interaction between subtype and injected current. Compete statistics are available in RESULTS. *B*: the slope of the evoked AP to depolarizing current injection curve is decreased in Drd1a-positive MSNs compared with Drd2-positive MSNs, with male MSNs exhibiting a larger difference between MSN subtypes than female MSNs. *C*: the delay to 1st AP evoked by rheobase current injection is decreased in Drd1a-positive MSNs compared with Drd2-positive MSNs and does not differ by sex. *D*: the maximum AP firing rate evoked at +0.10-nA injected current is decreased in Drd1a-positive MSNs compared with Drd2-positive MSNs, with male MSNs exhibiting a larger difference between MSN subtypes than female MSNs. FI slope: slope of the evoked action potential to depolarizing current injection curve; $*P < 0.05$; $**P < 0.01$; $***P < 0.001$.

female Drd1a-positive MSNs did not differ from any group, including female non-Drd1a MSNs ($P > 0.05$, $d = 0.31$). Capacitance, calculated as the time constant of the membrane divided by nonrectified range input resistance, did not differ between any group [male Drd1a: 60.7 ± 3.0 pF, female Drd1a: 67.3 ± 3.8, male Drd2: 60.1 ± 4.2, female Drd2: 60.6 ± 2.8; absolute values: subtype: $F_{(1,89)} = 1.18$, $P = 0.2811$; sex: $F_{(1,89)} = 1.09$, $P = 0.2988$; interaction: $F_{(1,89)} = 0.80$, $P = 0.3741$] Collectively, these data indicate that MSN passive membrane properties exhibit differences between subtypes and that male MSNs exhibit a larger effect size between subtypes than do female MSNs.

mEPSC properties. In a subset of recordings, we voltage clamped 22 male and 18 female Drd1a-positive MSNs and 18 male and 14 female Drd2-positive MSNs and recorded mEPSCs in the presence of TTX and PTX (Fig. 6*A*). We then analyzed mEPSC frequency, amplitude, and decay (Table 3). These experiments were inspired by previous work showing substantial increased mEPSC frequency in female compared with male AcbC MSNs in prepubertal and adult rats (Cao et al. 2016; Wissman et al. 2011). mEPSC frequency was increased in Drd1a-positive MSNs compared with Drd2-positive MSNs [Fig. 6*B*, *left*, absolute values: subtype: $F_{(1,68)} = 12.69$, $P = 0.0113$; sex: $F_{(1,68)} = 0.03$, $P = 0.8587$; interaction: $F_{(1,68)} = 6.79$, $P = 0.0113$] [Fig. 6*B*, *right*, normalized values: subtype: $F_{(1,68)} = 12.69$ $P = 0.0007$; sex: $F_{(1,68)} = 0.03$, $P = 0.8586$; interaction: $F_{(1,68)} = 6.82$, $P = 0.0111$]. Compared between groups, the mEPSC frequency of male Drd1a-positive MSNs differed from female Drd2-positive MSNs ($P < 0.05$, $d = 0.88$) but not male Drd2-positive MSNs ($P > 0.05$, $d = 0.23$). The mEPSC frequency of female Drd1a-positive MSNs differed from male Drd2-positive MSNs ($P < 0.05$, $d = 0.85$) and female Drd2-positive MSNs ($P < 0.001$, $d = 1.55$). Other mEPSC parameters also differed by subtype. mEPSC amplitude was increased in Drd1a-positive MSNs compared with Drd2-positive MSNs [Fig. 6*C*, *left*, absolute values: subtype: $F_{(1,68)} = 7.84$, $P = 0.0066$; sex: $F_{(1,68)} = 1.79$, $P = 0.1860$; interaction: $F_{(1,68)} = 0.03$, $P = 0.8609$] [Fig. 6*C*, *right*, normalized values: subtype: $F_{(1,68)} = 7.85$ $P = 0.0066$; sex: $F_{(1,68)} = 1.79$, $P = 0.1861$; interaction: $F_{(1,68)} = 0.03$, $P = 0.8609$]. Compared between groups, the mEPSC amplitude of male Drd1a-positive MSNs differed from female Drd2-positive MSNs ($P < 0.05$, $d = 0.96$) but not to male Drd2-positive MSNs ($P > 0.05$, $d = 0.57$) or any other group. The mEPSC amplitude of female Drd1a-positive MSNs differed from female Drd2-positive MSN ($P < 0.05$, $d = 0.89$). mEPSC decay was increased in Drd1a-positive MSNs compared with Drd2-positive MSNs [Fig. 6*D*, *left*, absolute values: subtype: $F_{(1,68)} = 22.34$, $P < 0.0001$; sex: $F_{(1,68)} = 0.88$, $P = 0.3523$; interaction: $F_{(1,68)} = 3.49$, $P = 0.0662$] [Fig. 6*D*, *right*, normalized values: subtype: $F_{(1,68)} = 22.34$, $P < 0.0001$; sex: $F_{(1,68)} = 0.87$, $P = 0.3523$; interaction: $F_{(1,68)} = 3.49$, $P = 0.0662$]. Compared between groups, the mEPSC amplitude of male Drd1a-positive MSNs differed from male and female Drd2-positive MSNs ($P < 0.05$, $d = 0.64$; $P < 0.001$, $d = 1.26$, respectively). Female Drd1a-positive MSNs differed from male and female Drd2-positive MSNs ($P < 0.05$, $d = 0.97$; $P < 0.001$, $d = 1.69$). These data indicate the mEPSC properties differ by MSN subtype and that female MSNs show a greater effect size between subtypes than do male MSNs but that prepubertal mice AcbC MSNs do not seem to exhibit the robust sex difference in mEPSC frequency detected in prepubertal rats.

DISCUSSION

These findings significantly extend the scientific literature examining MSN subtype electrophysiological properties, especially within the AcbC. To our knowledge this study is the most comprehensive assessment ever of AcbC MSN subtype electrophysiology and is the first to test whether any MSN subtype electrophysiological property differs between males and females in any striatal region or species. At this point it is well established that male MSN subtypes exhibit differential excitatory synaptic and intrinsic physiological properties (Table 4). In general, the Drd2-positive MSN subtype exhibits increased excitability compared with the Drd1a-positive MSN subtype (Gertler et al. 2008; Ma et al. 2012; Planert et al. 2013). Our study is consistent with these previous findings. For example, our study detected a strong difference in rheobase between MSN subtypes, with Drd1a-positive MSNs requiring a larger rheobase current to initiate an action potential compared with Drd2-positive MSNs in both males and females (Fig. 2*C*). This difference between MSN subtypes in rheobase and in other supportive electrophysiological metrics indicates that the foundational finding that MSN subtypes exhibit differences in excitability extends to both males and females.

Interestingly, there is a complex but patterned difference in effect sizes between MSN subtype electrophysiological properties between males and females, including those underlying neuronal excitability (Fig. 7). MSN subtype differences in action potential and membrane properties were more pronounced in male compared with female mice. This includes properties such as action potential width; the overall size of the action potential AHP, as indicated by the AHP peak amplitude, and the AHP time to peak amplitude; among others. Input resistance in the linear and rectified ranges, inward rectification, and the time constant of the membrane also showed increased effect size between MSN subtypes in males compared with females. This difference in effect size between male and female input resistance measurements may be a factor in why only select studies of MSN subtypes detect differences in input resistance. For example, Gertler et al. (2008) detected that the input resistance in Drd1a-positive MSNs was decreased compared with Drd2-positive MSN subtypes in the caudate-putamen of mice of unreported sex, as did Planert et al. (2013) in rats but not mice. If the previous studies were mixing male and female animals, as is likely with neuroscience studies using mice and, to a lesser extent, rats (Shansky and Woolley 2016; Will et al. 2017), then it is possible that some of the divergent results across studies of MSN subtypes are potentially explained by the difference in the effect size of MSN subtype electrophysiological properties between males and females. Conversely, MSN subtype differences in mEPSC frequency were much more pronounced in female compared with male mice. Several MSN subtype differences also demonstrated comparable effect size between males and females, including the resting membrane potential, action potential rheobase, and time to first action potential. Several possibilities potentially underlie these effect size differences. One possibility is that the difference in the robustness of the effect size differences between MSN subtypes is due to random chance.

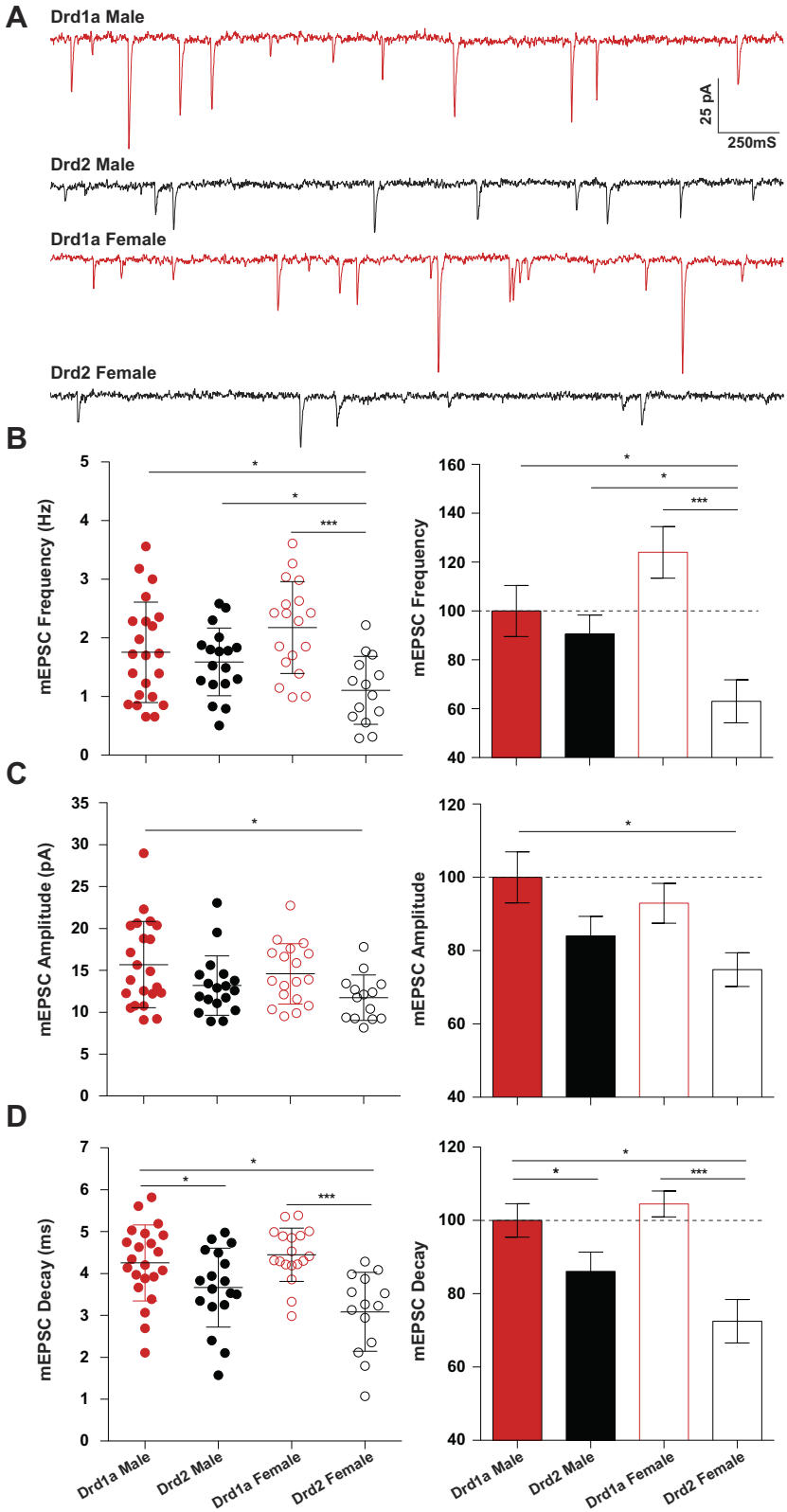

Fig. 6. Miniature excitatory postsynaptic current (mEPSC) properties vary by medium spiny neuron (MSN) subtype. *A*: mEPSCs recorded from male and female Drd1a-positive and Drd2-positive MSN subtypes. MSNs were voltage clamped at −70 mV and recorded in the presence of tetrodotoxin and picrotoxin to block voltage-gated sodium channels and GABAergic synaptic activity, respectively. *B*: mEPSC frequency was increased in Drd1a-positive MSNs compared with Drd2-positive MSNs, with female MSNs exhibiting a larger difference between MSN subtypes than male MSNs. *Left*: absolute values. Means ± SE are depicted over individual data points. *Right*: Values normalized to male Drd1a-positive MSNs. *C*: mEPSC amplitude is increased in Drd1a-positive MSNs compared with Drd2-positive MSNs, with female MSNs exhibiting a larger difference between MSN subtypes than male MSNs. *Left*: absolute values. *Right*: normalized values. *D*: mEPSC decay was increased in Drd1a-positive MSNs compared with Drd2-positive MSNs, with female MSNs exhibiting a larger difference between MSN subtypes than male MSNs. $*P < 0.05$; $***P < 0.001$.

We do not find this explanation particularly likely, as electrophysiological characteristics related to similar phenomenon (such as the action potential) show concerted changes. Another explanation is that there are sex differences in the expression of relevant proteins and receptors. Although both adult mouse and rat AcbC and other striatal regions express membrane estrogen receptors (ERs) such as GPER-1, membrane-associated ERα, and membrane-associated ERβ (Almey et al. 2012, 2015, 2016; Küppers and Beyer 1999; Mermelstein et al. 1996; Mitra et al. 2003), the relative expression levels of these receptors are

Table 3. *mEPSC properties of Drd1a- and Drd2-positive mouse medium spiny neurons*

MSN Subtype	mEPSC Amplitude, pA	mEPSC Decay, ms	mEPSC Frequency, Hz
Drd1a male (22)	15.69 ± 5.14[a]	4.25 ± 0.9[a]	1.76 ± 0.86[a]
Drd2 male (18)	13.19 ± 3.55[a,b]	3.66 ± 0.94[b,c]	1.59 ± 0.58[a]
Drd1a female (18)	14.58 ± 3.62[a,b]	4.45 ± 0.64[a,b]	2.18 ± 0.78[a]
Drd2 female (18)	11.74 ± 2.71[b]	3.08 ± 0.94[c]	1.11 ± 0.58[b]

Values are means ± SE. Numbers in parentheses indicate experimental "n." MSN, medium spiny neuron; mEPSC, miniature excitatory postsynaptic current. [a,b,c]Different superscript letters denote significant differences between groups within a column.

poorly documented, especially across developmental periods, strains, and adult female hormone cycles. Aromatase, the protein that metabolizes the sex steroid hormone testosterone into 17β-estradiol, is present in mouse and rat AcbC, but the exact details of its expression are likewise opaque (Foidart et al. 1995; Küppers and Beyer 1998; Stanić et al. 2014).

A different explanation is that the development of MSN subtype properties differs between males and females, at least in this particular transgenic mouse strain, and that eventually as the animals age the sex-specific differences in effect size of MSN subtype electrophysiological properties will converge. Studies of MSN electrophysiological development in the nucleus accumbens of rats shows that select MSN electrophysiological properties further develop between prepubertal and adult rats (Belleau and Warren 2000; Kasanetz and Manzoni 2009; Zhang and Warren 2008) and in both rats and mice dopamine receptors in the nucleus accumbens undergo significant developmental changes during adolescence (Andersen et al. 1997; Andersen and Teicher 2000). In contrast, Gertler et al. (2008) found that MSN subtype electrophysiological properties already differed prepuberty in the caudate-putamen in mice of unreported sex from a different transgenic line. Thus the differences in effect size between male and female MSN subtypes may either converge or further differentiate by adulthood, a possibility that should be addressed in future studies, along with the potential influence of the estrous cycle in adult females.

An important finding of this study is that mice AcbC MSNs do not exhibit the same sex differences in mEPSC frequency found in rat MSNs, including during the prepubertal developmental period assessed here (Cao et al. 2016; Wissman et al. 2011). In the rat, mEPSC frequency is elevated in both adult and prepubertal female compared with male AcbC MSNs. In this study, there were no sex differences detected in mEPSC frequency, although an interaction effect indicated that female Drd2-positive MSNs exhibited a lower mEPSC frequency compared with other groups. There were also no sex differences detected in intrinsic excitability and action potential properties, similar to previous findings in prepubertal rat AcbC (Cao et al. 2016), nucleus accumbens shell (Willett et al. 2016) but not caudate-putamen (Dorris et al. 2015). This general lack of effect of sex could be due to several causes. First, as mentioned previously, the developmental trajectory of mice may differ than that of rats, and a caveat of the current study is its focus on the prepubertal period. In rats, sex differences in AcbC excitatory synapse properties exist before puberty and are sensitive to neonatal sex steroid hormone exposure (Cao et al. 2016). Adult rats likewise exhibit sex differences in AcbC excitatory glutamatergic synapse properties (Forlano and Woolley 2010; Wissman et al. 2011, 2012), although the role of the estrous cycle and puberty in altering AcbC synaptic properties is relatively unexplored. For these reasons, along with anecdotal evidence that most neurophysiological experiments occur in prepubertal animals (Moyer and Brown 1998), we chose to target the P16–24 age range for this study. This age range is past the perinatal critical period for masculinization/defeminization via sex steroid hormone exposure and is within the age range during which prepubertal sex differences in excitatory synaptic input were detected in rat AcbC MSNs (Cao et al. 2016) and in intrinsic excitability in rat caudate-putamen MSNs (Dorris et al. 2015). Several AcbC-mediated behaviors that have been primarily assessed in rats are sensitive to neonatal sex steroid hormone exposure and/or show sex differences before puberty, for example, impulsivity, social play, and cocaine self-administration behaviors (Bayless et al. 2013; Blake and McCoy 2015; Perry et al. 2013). However, other relevant behaviors are sensitive to pubertal and adult processes (Yoest et al. 2018), including social play and vulnerability to social stress during puberty in mice (Fosnocht et al. 2018; Kopec et al. 2017). Thus it remains possible that sex differences in AcbC excitatory synaptic input may be detected in older populations of mice. It is also possible that sex differences may exist in cellular metrics not assessed by this study, including dendritic spine attributes. Regarding other caveats, the current study conducted electrophysiological recordings at room temperature, and it is possible that sex differences could emerge if a different recording temperature was employed. Sex differences may also exist in MSN electrophysiological properties in other striatal regions than the nucleus accumbens core, including the caudate-putamen and nucleus accumbens shell, and in animals exposed to stress and other environmental stimuli (Brancato et al. 2017).

Other reasons why the mouse strain assessed here did not exhibit the same sex differences as do rats may be due to ethological differences, the possible disruptive effects of transgene insertion, the effects of substantial inbreeding, and/or domestication. To focus specifically on female mice, alteration of female inbred mouse AcbC function compared with outbred rodent strains may have occurred because generations of domestication in laboratory mice have focused on artificially selecting reproductive traits in mice that enable ease of breeding in the laboratory with any presented male, early sexual maturity, and large litter size (Austad 2002). Indeed, inbred laboratory mice are artificially selected to ensure maximal reproduction within a laboratory setting (Perlman 2016). This artificial selection may have altered the physiological mechanisms of sexual reward in inbred, domesticated mice. Sophisticated genetic and behavioral analyses indicate that domestication more highly impacts female than male inbred mice, with female mice losing numerous sex-relevant behaviors found in wild, nondomesticated mice (Chalfin et al. 2014). This loss of sex-relevant behaviors is consistent with the absence of sex differences in AcbC MSN mEPSC frequency detected by the current study, especially as the AcbC mediates sexual reward, along with other naturally rewarding behaviors (Bradley et al. 2005; Frohmader et al. 2010; Numan 2007; Young et al. 2011). Sex differences in the properties of the nucleus accumbens are thought to be driven by neural circuity inducing an increased

Table 4. *Differential electrophysiological properties of medium spiny neuron subtypes across striatal regions, species, and studies*

Striatal Region	Species, Strain, Age and Sex	Measurement	References
Nucleus accumbens core	D1 and D2 receptor-eGFP BAC transgenic mice on a FVB/N background; Older than P28, 42.9 ± 2.2; sex not reported	Time constant of the membrane: D1 < D2 Rheobase: D1 > D2Resting membrane potential: D1 < D2 I_h amplitude: D1 > D2 sEPSC frequency: D1 < D2	(Ma et al. 2012)
Nucleus Accumbens core	B6 *Cg-Tg (Drd1a*-tdTomato) 6 Calak/J hemizygous mice on a C57BL/6J background; P16–24; male and female	Resting membrane potential: D1 < D2 Rheobase: D1 > D2 Action potential width: D1 < D2 (males only) Afterhyperpolarization peak amplitude: D1 < D2 (males only) Afterhyperpolarization time to peak amplitude: D1 > D2 (males only) Frequency of action potentials evoked by injected current: D1 < D2 Slope of the frequency of action potentials evoked by injected current curve: D1 < D2 (males only) Delay to first action potential: D1 < D2 Maximum firing rate: D1 < D2 (males only) Input resistance, linear range: D1 < D2 (males only) Input resistance, rectified range: D1 < D2 (males only) Inward rectification: D1 < D2 (males only) Time constant of the membrane: D1 < D2 (males only) mEPSC frequency: D1 > D2 (females only) mEPSC decay: D1 > D2	Current Study
Nucleus accumbens shell	D1 and D2 receptor-eGFP BAC transgenic mice on a FVB/N background; older than P28, 42.9 ± 2.2; sex not reported	Time constant of the membrane: D1 > D2 sEPSC Frequency: D1 < D2	(Ma et al. 2012)
Caudate-putamen	D1 and D2 receptor-eGFP BAC transgenic mice on an FVB background; P17-P70; sex not reported	Rheobase: D1 > D2 Resting membrane potential: D1 < D2 Input Resistance (linear range): D1 < D2 Time constant of the membrane: D1 > D2 Frequency of Evoked Action Potentials: D1 < D2 Capacitance: D1 > D2	(Gertler et al. 2008)
Caudate-putamen	D1 and D2 receptor-eGFP BAC transgenic mice; older than P28: 39.7 ± 1.6; sex not reported	Threshold: D1 > D2 sEPSC frequency: D1 < D2 mEPSC frequency: D1 < D2[a] mEPSC rise time: D1 < D2 Probability of occurrence of spontaneous membrane depolarization after $GABA_A$ blockade: D1 < D2 Paired-pulse ratio: D1 < D2 AMPA-induced current amplitude: D1 > D2	(Cepeda et al. 2008)
Caudate-putamen	D1 receptor-eGFP BAC transgenic mice; P15, 21–32; sex not reported	Rheobase[b]: D1 > D2	(Planert et al. 2013)
Caudate-putamen	Sprague-Dawley Rat; P14–19; sex not reported	Rheobase: D1 > D2 Time constant of the membrane: D1 < D2 Input resistance: D1 < D2 AP amplitude change from first to second AP: D1 > D2	(Planert et al. 2013)
Caudate-putamen	D1 and D2 receptor-eGFP BAC transgenic mice on either a FVB/NJ or C57BL/6J background; P21-P35; males	Excitability as measured via evoked AP to intensity of injected current curves: D1 < D2	(Chan et al. 2012)
Caudate-Putamen	M4- or D2-eGFP BAC transgenic mice[c]; P20–25; sex not reported	Paired-pulse ratio: D1 > D2 mEPSC frequency: D1 < D2 NMDA/AMPA ratio: D1 < D2 Frequency of action potentials evoked by injected current: D1 < D2 Endocannabinoid-mediated LTD: D1 < D2	(Kreitzer and Malenka 2007)
Caudate-Putamen	D1 and D2 receptor-eGFP BAC transgenic mice on a C57BL/6J background; P16-P25; male and female but data not analyzed by sex	Tonic $GABA_A$ current and sensitivity to $GABA_A$ current: D1 < D2 Frequency of action potentials evoked by injected current: D1 < D2	(Ade et al. 2008)[d]

Only statistically significant differences in medium spiny neuron (MSN) electrophysiology in acute brain slice technique experiments independent of variables such as stress and psychostimulant exposure are included. This criteria a priori excludes studies that analyzed MSN subtype electrophysiological properties but did not directly compare D1 and D2 subtype groups, for example, Francis et al. (2015); Khibnik et al. (2016); and Kim et al. (2011). BAC, bacterial artificial chromosome; sEPSC and mEPSC, spontaneous and miniature excitatory postsynaptic current; AP, action potential; P, postnatal day; I_h, hyperpolarization-induced "sag." [a]This finding significant in some but not all analyses within this study. [b]Planert et al. (2013) assessed rheobase using multiple analyses. The conclusion of all analyses was similar and is thus condensed here. [c]The use of M4 eGFP labeling as equivalent to the D1 MSN subtype has been cautioned (Cepeda et al. 2008). [d]A number of studies from Vicini and colleagues (2008) have investigated GABA conductance between MSN subtypes; here we feature the initial report.

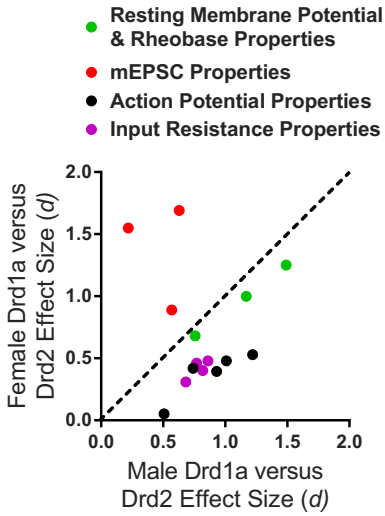

Fig. 7. Comparison of medium spiny neuron (MSN) subtype electrophysiological property effect sizes between females and males. Each point represents the Cohen's *d* value calculated for 1 of the 15 electrophysiological properties that significantly differ between Drd1a- and Drd2-positive female and male MSN subtypes. The dashed line is the unity line. Points on or near the unity line indicate that effect size is comparable between male and female MSN. Points located above the unity line indicate a larger effect size in female MSNs. Points located below the unity line indicate a larger effect size in male MSNs. Female MSNs showed larger differences in MSN subtype electrophysiological properties in miniature excitatory postsynaptic current (mEPSC) properties. Conversely, male MSNs showed larger differences in MSN subtype electrophysiological properties in action potential and input resistance properties.

motivation for sexual reward (Micevych and Meisel 2017; Tonn Eisinger et al. 2018). There is evidence that the domestication of laboratory mice has disrupted select nucleus accumbens-relevant locomotor, social, and reproductive behaviors (Blanchard et al. 1998; Guénet and Bonhomme 2003; Harper 2008; Price 1984; Sherborne et al. 2007). Likewise, some drug-abuse and other motivation-related behaviors mediated by the nucleus accumbens that show sex differences and estrogen and progesterone sensitivity are impossible or highly difficult to induce in mice (Parker et al. 2014), although this has been in many instances mitigated (Calipari et al. 2017; Satta et al. 2017).

The insertion of transgenes could also potentially alter sexual differentiation and AcbC-mediated behaviors, particularly when homozygosity and strain are not carefully controlled. For example, homozygous Drd2-expressing BAC transgenic mice on specific backgrounds show aberrant striatal-mediated locomotor behaviors (Kramer et al. 2011), and the line 5 of the tdTomato-drd1a transgenic mouse showed aberrant properties that negatively impacted its utility for sex and hormone research, including an X-linked inheritance pattern and ambiguous mammary glands (Ade et al. 2011; Shuen et al. 2008). Line 6 of the tdTomato-drd1a transgenic mouse does not exhibit these obvious confounds. However, it remains formally possible that the addition of transgenes targeting dopamine receptors subtly disrupts the sexual differentiation of the AcbC, as this would impact reproduction-related behaviors not typically assessed in the standard characterization of transgenic mouse lines. Please note that these potential caveats do not dismiss transgenic laboratory mice as important tools for research into AcbC function, reproductive behavior, and sexual differentiation. Indeed, mouse models such as the four core genotypes have made critical contributions to our understanding of the influence of biological sex on neural systems (De Vries et al. 2002), including the limbic brain regions (Bath et al. 2017; Puralewski et al. 2016). What these caveats do argue, along with this study's finding that mouse AcbC MSNs do not show the same sex differences as detected in rat AcbC MSNs, is that both the advantages and disadvantages of particular research animals should be carefully considered, especially in the context of assessing natural variables in neuron function such as sex and sex steroid hormone sensitivity. Future studies should continue to address the impact of biological sex and steroid sex hormones in AcbC properties across a broad array of inbred and outbred animals with divergent reproductive strategies, similar to suggestions made by other authors in diverse research contexts (Beach 1950; Brenowitz and Zakon 2015; Klinck et al. 2017; Krebs 1975; Remage-Healey et al. 2017).

ACKNOWLEDGMENTS

We thank Jaime Willett and Stephanie Proaño for technical support, Dr. Amanda Krentzel for critiquing an earlier version of this manuscript, Drs. Jonathan Ting, David Aylor, Heather Patisaul, and Scott Belcher for advice regarding mice selection, breeding, and data analysis,

GRANTS

We also thank the following for being funding sources: Army Research Office STIR Award W911NF-15-1-0476, National Center on Minority Health and Health Disparities Grant R01-MH-109471 (to J. Meitzen), North Carolina State University Start-up Funds (to J. Meitzen) and (Center for Human Health and the Environment Grant P30ES025128.

DISCLOSURES

No conflicts of interest, financial or otherwise, are declared by the authors.

AUTHOR CONTRIBUTIONS

J.C. and J.M. conceived and designed research; J.C. performed experiments; J.C., D.M.D., and J.M. analyzed data; J.C. and J.M. interpreted results of experiments; J.C., D.M.D., and J.M. prepared figures; J.C. and J.M. drafted manuscript; J.C., D.M.D., and J.M. edited and revised manuscript; J.C., D.M.D., and J.M. approved final version of manuscript.

REFERENCES

Ade KK, Janssen MJ, Ortinski PI, Vicini S. Differential tonic GABA conductances in striatal medium spiny neurons. *J Neurosci* 28: 1185–1197, 2008. doi:10.1523/JNEUROSCI.3908-07.2008.

Ade KK, Wan Y, Chen M, Gloss B, Calakos N. An improved BAC transgenic fluorescent reporter line for sensitive and specific identification of striatonigral medium spiny neurons. *Front Syst Neurosci* 5: 32, 2011. doi:10.3389/fnsys.2011.00032.

Almey A, Filardo EJ, Milner TA, Brake WG. Estrogen receptors are found in glia and at extranuclear neuronal sites in the dorsal striatum of female rats: evidence for cholinergic but not dopaminergic colocalization. *Endocrinology* 153: 5373–5383, 2012. doi:10.1210/en.2012-1458.

Almey A, Milner TA, Brake WG. Estrogen receptors in the central nervous system and their implication for dopamine-dependent cognition in females. *Horm Behav* 74: 125–138, 2015. doi:10.1016/j.yhbeh.2015.06.010.

Almey A, Milner TA, Brake WG. Estrogen receptor α and G-protein coupled estrogen receptor 1 are localized to GABAergic neurons in the dorsal striatum. *Neurosci Lett* 622: 118–123, 2016. doi:10.1016/j.neulet.2016.04.023.

Andersen SL, Rutstein M, Benzo JM, Hostetter JC, Teicher MH. Sex differences in dopamine receptor overproduction and elimination. *Neuroreport* 8: 1495–1498, 1997. doi:10.1097/00001756-199704140-00034.

Andersen SL, Teicher MH. Sex differences in dopamine receptors and their relevance to ADHD. *Neurosci Biobehav Rev* 24: 137–141, 2000. doi:10.1016/S0149-7634(99)00044-5.

Austad SN. A mouse's tale. *Nat Hist* 111: 64–70, 2002.

Bath KG, Russo SJ, Pleil KE, Wohleb ES, Duman RS, Radley JJ. Circuit and synaptic mechanisms of repeated stress: Perspectives from differing contexts, duration, and development. *Neurobiol Stress* 7: 137–151, 2017. doi:10.1016/j.ynstr.2017.05.001.

Baufreton J, Atherton JF, Surmeier DJ, Bevan MD. Enhancement of excitatory synaptic integration by GABAergic inhibition in the subthalamic nucleus. *J Neurosci* 25: 8505–8517, 2005. doi:10.1523/JNEUROSCI.1163-05.2005.

Bayless DW, Darling JS, Daniel JM. Mechanisms by which neonatal testosterone exposure mediates sex differences in impulsivity in prepubertal rats. *Horm Behav* 64: 764–769, 2013. doi:10.1016/j.yhbeh.2013.10.003.

Beach FA. The snark was a boojum. *Am Psychol* 5: 115–124, 1950. doi:10.1037/h0056510.

Becker JB, Hu M. Sex differences in drug abuse. *Front Neuroendocrinol* 29: 36–47, 2008. doi:10.1016/j.yfrne.2007.07.003.

Becker JB, Koob GF. Sex differences in animal models: focus on addiction. *Pharmacol Rev* 68: 242–263, 2016. doi:10.1124/pr.115.011163.

Beery AK, Zucker I. Sex bias in neuroscience and biomedical research. *Neurosci Biobehav Rev* 35: 565–572, 2011. doi:10.1016/j.neubiorev.2010.07.002.

Belleau ML, Warren RA. Postnatal development of electrophysiological properties of nucleus accumbens neurons. *J Neurophysiol* 84: 2204–2216, 2000. doi:10.1152/jn.2000.84.5.2204.

Blake BE, McCoy KA. Hormonal programming of rat social play behavior: Standardized techniques will aid synthesis and translation to human health. *Neurosci Biobehav Rev* 55: 184–197, 2015. doi:10.1016/j.neubiorev.2015.04.021.

Blanchard RJ, Hebert MA, Ferrari PF, Palanza P, Figueira R, Blanchard DC, Parmigiani S. Defensive behaviors in wild and laboratory (Swiss) mice: the mouse defense test battery. *Physiol Behav* 65: 201–209, 1998. doi:10.1016/S0031-9384(98)00012-2.

Bradley KC, Boulware MB, Jiang H, Doerge RW, Meisel RL, Mermelstein PG. Changes in gene expression within the nucleus accumbens and striatum following sexual experience. *Genes Brain Behav* 4: 31–44, 2005. doi:10.1111/j.1601-183X.2004.00093.x.

Brancato A, Bregman D, Ahn HF, Pfau ML, Menard C, Cannizzaro C, Russo SJ, Hodes GE. Sub-chronic variable stress induces sex-specific effects on glutamatergic synapses in the nucleus accumbens. *Neuroscience* 350: 180–189, 2017. doi:10.1016/j.neuroscience.2017.03.014.

Brenowitz EA, Zakon HH. Emerging from the bottleneck: benefits of the comparative approach to modern neuroscience. *Trends Neurosci* 38: 273–278, 2015. doi:10.1016/j.tins.2015.02.008.

Calipari ES, Juarez B, Morel C, Walker DM, Cahill ME, Ribeiro E, Roman-Ortiz C, Ramakrishnan C, Deisseroth K, Han MH, Nestler EJ. Dopaminergic dynamics underlying sex-specific cocaine reward. *Nat Commun* 8: 13877, 2017. doi:10.1038/ncomms13877.

Cao J, Dorris DM, Meitzen J. Neonatal masculinization blocks increased excitatory synaptic input in female rat nucleus accumbens core. *Endocrinology* 157: 3181–3196, 2016. doi:10.1210/en.2016-1160.

Carroll ME, Anker JJ. Sex differences and ovarian hormones in animal models of drug dependence. *Horm Behav* 58: 44–56, 2010. doi:10.1016/j.yhbeh.2009.10.001.

Cepeda C, André VM, Yamazaki I, Wu N, Kleiman-Weiner M, Levine MS. Differential electrophysiological properties of dopamine D1 and D2 receptor-containing striatal medium-sized spiny neurons. *Eur J Neurosci* 27: 671–682, 2008. doi:10.1111/j.1460-9568.2008.06038.x.

Chalfin L, Dayan M, Levy DR, Austad SN, Miller RA, Iraqi FA, Dulac C, Kimchi T. Mapping ecologically relevant social behaviours by gene knockout in wild mice. *Nat Commun* 5: 4569, 2014. doi:10.1038/ncomms5569.

Chan CS, Peterson JD, Gertler TS, Glajch KE, Quintana RE, Cui Q, Sebel LE, Plotkin JL, Shen W, Heiman M, Heintz N, Greengard P, Surmeier DJ. Strain-specific regulation of striatal phenotype in Drd2-eGFP BAC transgenic mice. *J Neurosci* 32: 9124–9132, 2012. doi:10.1523/JNEUROSCI.0229-12.2012.

Cohen J. *Statistical Power Analysis for the Behavioral Sciences* (rev. ed.). Hillsdale, NJ: Erlbaum, 1977.

De Vries GJ, Rissman EF, Simerly RB, Yang LY, Scordalakes EM, Auger CJ, Swain A, Lovell-Badge R, Burgoyne PS, Arnold AP. A model system for study of sex chromosome effects on sexually dimorphic neural and behavioral traits. *J Neurosci* 22: 9005–9014, 2002. doi:10.1523/JNEUROSCI.22-20-09005.2002.

Di Paolo T. Modulation of brain dopamine transmission by sex steroids. *Rev Neurosci* 5: 27–41, 1994. doi:10.1515/REVNEURO.1994.5.1.27.

Dorris DM, Cao J, Willett JA, Hauser CA, Meitzen J. Intrinsic excitability varies by sex in prepubertal striatal medium spiny neurons. *J Neurophysiol* 113: 720–729, 2015. doi:10.1152/jn.00687.2014.

Dorris DM, Hauser CA, Minnehan CE, Meitzen J. An aerator for brain slice experiments in individual cell culture plate wells. *J Neurosci Methods* 238: 1–10, 2014. doi:10.1016/j.jneumeth.2014.09.017.

Enoksson T, Bertran-Gonzalez J, Christie MJ. Nucleus accumbens D2- and D1-receptor expressing medium spiny neurons are selectively activated by morphine withdrawal and acute morphine, respectively. *Neuropharmacology* 62: 2463–2471, 2012. doi:10.1016/j.neuropharm.2012.02.020.

Farries MA, Meitzen J, Perkel DJ. Electrophysiological properties of neurons in the basal ganglia of the domestic chick: conservation and divergence in the evolution of the avian basal ganglia. *J Neurophysiol* 94: 454–467, 2005. doi:10.1152/jn.00539.2004.

Farries MA, Perkel DJ. Electrophysiological properties of avian basal ganglia neurons recorded in vitro. *J Neurophysiol* 84: 2502–2513, 2000. doi:10.1152/jn.2000.84.5.2502.

Farries MA, Perkel DJ. A telencephalic nucleus essential for song learning contains neurons with physiological characteristics of both striatum and globus pallidus. *J Neurosci* 22: 3776–3787, 2002. doi:10.1523/JNEUROSCI.22-09-03776.2002.

Fieblinger T, Graves SM, Sebel LE, Alcacer C, Plotkin JL, Gertler TS, Chan CS, Heiman M, Greengard P, Cenci MA, Surmeier DJ. Cell type-specific plasticity of striatal projection neurons in parkinsonism and L-DOPA-induced dyskinesia. *Nat Commun* 5: 5316, 2014. doi:10.1038/ncomms6316.

Foidart A, Harada N, Balthazart J. Aromatase-immunoreactive cells are present in mouse brain areas that are known to express high levels of aromatase activity. *Cell Tissue Res* 280: 561–574, 1995. doi:10.1007/BF00318360.

Forlano PM, Woolley CS. Quantitative analysis of pre- and postsynaptic sex differences in the nucleus accumbens. *J Comp Neurol* 518: 1330–1348, 2010. doi:10.1002/cne.22279.

Fosnocht AQ, Lucerne KE, Ellis AS, Olimpo NA, Briand LA. Adolescent social isolation increases vulnerability to cocaine. *BioRxiv* 320648, 2018. doi:10.1101/320648.

Francis TC, Chandra R, Friend DM, Finkel E, Dayrit G, Miranda J, Brooks JM, Iñiguez SD, O'Donnell P, Kravitz A, Lobo MK. Nucleus accumbens medium spiny neuron subtypes mediate depression-related outcomes to social defeat stress. *Biol Psychiatry* 77: 212–222, 2015. doi:10.1016/j.biopsych.2014.07.021.

Francis TC, Lobo MK. Emerging role for nucleus accumbens medium spiny neuron subtypes in depression. *Biol Psychiatry* 81: 645–653, 2017. doi:10.1016/j.biopsych.2016.09.007.

Friend DM, Kravitz AV. Working together: basal ganglia pathways in action selection. *Trends Neurosci* 37: 301–303, 2014. doi:10.1016/j.tins.2014.04.004.

Frohmader KS, Pitchers KK, Balfour ME, Coolen LM. Mixing pleasures: review of the effects of drugs on sex behavior in humans and animal models. *Horm Behav* 58: 149–162, 2010. doi:10.1016/j.yhbeh.2009.11.009.

Gerfen CR. The neostriatal mosaic: multiple levels of compartmental organization. *Trends Neurosci* 15: 133–139, 1992. doi:10.1016/0166-2236(92)90355-C.

Gerfen CR, Engber TM, Mahan LC, Susel Z, Chase TN, Monsma FJ Jr, Sibley DR. D1 and D2 dopamine receptor-regulated gene expression of striatonigral and striatopallidal neurons. *Science* 250: 1429–1432, 1990. doi:10.1126/science.2147780.

Gertler TS, Chan CS, Surmeier DJ. Dichotomous anatomical properties of adult striatal medium spiny neurons. *J Neurosci* 28: 10814–10824, 2008. doi:10.1523/JNEUROSCI.2660-08.2008.

Groenewegen HJ, Wright CI, Beijer AV, Voorn P. Convergence and segregation of ventral striatal inputs and outputs. *Ann NY Acad Sci* 877: 49–63, 1999. doi:10.1111/j.1749-6632.1999.tb09260.x.

Guénet JL, Bonhomme F. Wild mice: an ever-increasing contribution to a popular mammalian model. *Trends Genet* 19: 24–31, 2003. doi:10.1016/S0168-9525(02)00007-0.

Harper JM. Wild-derived mouse stocks: an underappreciated tool for aging research. *Age (Dordr)* 30: 135–145, 2008. doi:10.1007/s11357-008-9057-0.

Kasanetz F, Manzoni OJ. Maturation of excitatory synaptic transmission of the rat nucleus accumbens from juvenile to adult. *J Neurophysiol* 101: 2516–2527, 2009. doi:10.1152/jn.91039.2008.

Kelley AE. Ventral striatal control of appetitive motivation: role in ingestive behavior and reward-related learning. *Neurosci Biobehav Rev* 27: 765–776, 2004. doi:10.1016/j.neubiorev.2003.11.015.

Khibnik LA, Beaumont M, Doyle M, Heshmati M, Slesinger PA, Nestler EJ, Russo SJ. Stress and cocaine trigger divergent and cell type-specific regulation of synaptic transmission at single spines in nucleus accumbens. *Biol Psychiatry* 79: 898–905, 2016. doi:10.1016/j.biopsych.2015.05.022.

Kim J, Park BH, Lee JH, Park SK, Kim JH. Cell type-specific alterations in the nucleus accumbens by repeated exposures to cocaine. *Biol Psychiatry* 69: 1026–1034, 2011. doi:10.1016/j.biopsych.2011.01.013.

Klinck MP, Mogil JS, Moreau M, Lascelles BD, Flecknell PA, Poitte T, Troncy E. Translational pain assessment: could natural animal models be the missing link? *Pain* 158: 1633–1646, 2017. doi:10.1097/j.pain.0000000000000978.

Kopec A, Smith DJ, Aryre NR, Sweat SC, Bilbo SD. Microglial elimination of dopamine D1 receptors defines sex-specific changes in nucleus accumbens development and social play behavior during adolescence. *BioRxiv* 211029, 2017. doi:10.1101/211029.

Kramer PF, Christensen CH, Hazelwood LA, Dobi A, Bock R, Sibley DR, Mateo Y, Alvarez VA. Dopamine D2 receptor overexpression alters behavior and physiology in Drd2-EGFP mice. *J Neurosci* 31: 126–132, 2011. doi:10.1523/JNEUROSCI.4287-10.2011.

Krebs HA. The August Krogh Principle: "For many problems there is an animal on which it can be most conveniently studied". *J Exp Zool* 194: 221–226, 1975. doi:10.1002/jez.1401940115.

Kreitzer AC, Berke JD. Investigating striatal function through cell-type-specific manipulations. *Neuroscience* 198: 19–26, 2011. doi:10.1016/j.neuroscience.2011.08.018.

Kreitzer AC, Malenka RC. Endocannabinoid-mediated rescue of striatal LTD and motor deficits in Parkinson's disease models. *Nature* 445: 643–647, 2007. doi:10.1038/nature05506.

Kupchik YM, Brown RM, Heinsbroek JA, Lobo MK, Schwartz DJ, Kalivas PW. Coding the direct/indirect pathways by D1 and D2 receptors is not valid for accumbens projections. *Nat Neurosci* 18: 1230–1232, 2015. doi:10.1038/nn.4068.

Küppers E, Beyer C. Expression of aromatase in the embryonic and postnatal mouse striatum. *Brain Res Mol Brain Res* 63: 184–188, 1998. doi:10.1016/S0169-328X(98)00279-4.

Küppers E, Beyer C. Expression of estrogen receptor-alpha and beta mRNA in the developing and adult mouse striatum. *Neurosci Lett* 276: 95–98, 1999. doi:10.1016/S0304-3940(99)00815-0.

Lobo MK, Nestler EJ. The striatal balancing act in drug addiction: distinct roles of direct and indirect pathway medium spiny neurons. *Front Neuroanat* 5: 41, 2011. doi:10.3389/fnana.2011.00041.

Ma YY, Cepeda C, Chatta P, Franklin L, Evans CJ, Levine MS. Regional and cell-type-specific effects of DAMGO on striatal D1 and D2 dopamine receptor-expressing medium-sized spiny neurons. *ASN Neuro* 4: e00077, 2012. doi:10.1042/AN20110063.

Ma YY, Henley SM, Toll J, Jentsch JD, Evans CJ, Levine MS, Cepeda C. Drug-primed reinstatement of cocaine seeking in mice: increased excitability of medium-sized spiny neurons in the nucleus accumbens. *ASN Neuro* 5: 257–271, 2013. doi:10.1042/AN20130015.

Mani SK, Reyna AM, Alejandro MA, Crowley J, Markaverich BM. Disruption of male sexual behavior in rats by tetrahydrofurandiols (THF-diols). *Steroids* 70: 750–754, 2005. doi:10.1016/j.steroids.2005.04.004.

Markaverich B, Mani S, Alejandro MA, Mitchell A, Markaverich D, Brown T, Velez-Trippe C, Murchison C, O'Malley B, Faith R. A novel endocrine-disrupting agent in corn with mitogenic activity in human breast and prostatic cancer cells. *Environ Health Perspect* 110: 169–177, 2002. doi:10.1289/ehp.02110169.

McLean CP, Anderson ER. Brave men and timid women? A review of the gender differences in fear and anxiety. *Clin Psychol Rev* 29: 496–505, 2009. doi:10.1016/j.cpr.2009.05.003.

Meitzen J, Pflepsen KR, Stern CM, Meisel RL, Mermelstein PG. Measurements of neuron soma size and density in rat dorsal striatum, nucleus accumbens core and nucleus accumbens shell: differences between striatal region and brain hemisphere, but not sex. *Neurosci Lett* 487: 177–181, 2011. doi:10.1016/j.neulet.2010.10.017.

Meitzen J, Weaver AL, Brenowitz EA, Perkel DJ. Plastic and stable electrophysiological properties of adult avian forebrain song-control neurons across changing breeding conditions. *J Neurosci* 29: 6558–6567, 2009. doi:10.1523/JNEUROSCI.5571-08.2009.

Mermelstein PG, Becker JB, Surmeier DJ. Estradiol reduces calcium currents in rat neostriatal neurons via a membrane receptor. *J Neurosci* 16: 595–604, 1996. doi:10.1523/JNEUROSCI.16-02-00595.1996.

Mermelstein PG, Song WJ, Tkatch T, Yan Z, Surmeier DJ. Inwardly rectifying potassium (IRK) currents are correlated with IRK subunit expression in rat nucleus accumbens medium spiny neurons. *J Neurosci* 18: 6650–6661, 1998. doi:10.1523/JNEUROSCI.18-17-06650.1998.

Micevych PE, Meisel RL. Integrating neural circuits controlling female sexual behavior. *Front Syst Neurosci* 11: 42, 2017. doi:10.3389/fnsys.2017.00042.

Mitra SW, Hoskin E, Yudkovitz J, Pear L, Wilkinson HA, Hayashi S, Pfaff DW, Ogawa S, Rohrer SP, Schaeffer JM, McEwen BS, Alves SE. Immunolocalization of estrogen receptor beta in the mouse brain: comparison with estrogen receptor alpha. *Endocrinology* 144: 2055–2067, 2003. doi:10.1210/en.2002-221069.

Mogenson GJ, Jones DL, Yim CY. From motivation to action: functional interface between the limbic system and the motor system. *Prog Neurobiol* 14: 69–97, 1980. doi:10.1016/0301-0082(80)90018-0.

Morrison SE, McGinty VB, du Hoffmann J, Nicola SM. Limbic-motor integration by neural excitations and inhibitions in the nucleus accumbens. *J Neurophysiol* 118: 2549–2567, 2017. doi:10.1152/jn.00465.2017.

Moyer JR, Brown TH. Methods for whole-cell recording from visually preselected neurons of perirhinal cortex in brain slices from young and aging rats. *J Neurosci Methods* 86: 35–54, 1998. doi:10.1016/S0165-0270(98)00143-5.

Mu P, Moyer JT, Ishikawa M, Zhang Y, Panksepp J, Sorg BA, Schlüter OM, Dong Y. Exposure to cocaine dynamically regulates the intrinsic membrane excitability of nucleus accumbens neurons. *J Neurosci* 30: 3689–3699, 2010. doi:10.1523/JNEUROSCI.4063-09.2010.

Nicola SM. The nucleus accumbens as part of a basal ganglia action selection circuit. *Psychopharmacology (Berl)* 191: 521–550, 2007. doi:10.1007/s00213-006-0510-4.

Nisenbaum ES, Xu ZC, Wilson CJ. Contribution of a slowly inactivating potassium current to the transition to firing of neostriatal spiny projection neurons. *J Neurophysiol* 71: 1174–1189, 1994. doi:10.1152/jn.1994.71.3.1174.

Numan M. Motivational systems and the neural circuitry of maternal behavior in the rat. *Dev Psychobiol* 49: 12–21, 2007. doi:10.1002/dev.20198.

O'Donnell P, Grace AA. Physiological and morphological properties of accumbens core and shell neurons recorded in vitro. *Synapse* 13: 135–160, 1993. doi:10.1002/syn.890130206.

Parker CC, Chen H, Flagel SB, Geurts AM, Richards JB, Robinson TE, Solberg Woods LC, Palmer AA. Rats are the smart choice: Rationale for a renewed focus on rats in behavioral genetics. *Neuropharmacology* 76: 250–258, 2014. doi:10.1016/j.neuropharm.2013.05.047.

Perlman RL. Mouse models of human disease: an evolutionary perspective. *Evol Med Public Health* 2016: 170–176, 2016.

Perry AN, Westenbroek C, Becker JB. Impact of pubertal and adult estradiol treatments on cocaine self-administration. *Horm Behav* 64: 573–578, 2013. doi:10.1016/j.yhbeh.2013.08.007.

Peterson BM, Martinez LA, Meisel RL, Mermelstein PG. Estradiol impacts the endocannabinoid system in female rats to influence behavioral and structural responses to cocaine. *Neuropharmacology* 110: 118–124, 2016. doi:10.1016/j.neuropharm.2016.06.002.

Peterson BM, Mermelstein PG, Meisel RL. Estradiol mediates dendritic spine plasticity in the nucleus accumbens core through activation of mGluR5. *Brain Struct Funct* 220: 2415–2422, 2015. doi:10.1007/s00429-014-0794-9.

Planert H, Berger TK, Silberberg G. Membrane properties of striatal direct and indirect pathway neurons in mouse and rat slices and their modulation by dopamine. *PLoS One* 8: e57054, 2013. doi:10.1371/journal.pone.0057054.

Price EO. Behavioral-aspects of animal domestication. *Q Rev Biol* 59: 1–32, 1984. doi:10.1086/413673.

Puralewski R, Vasilakis G, Seney ML. Sex-related factors influence expression of mood-related genes in the basolateral amygdala differentially depending on age and stress exposure. *Biol Sex Differ* 7: 50, 2016. doi:10.1186/s13293-016-0106-6.

Remage-Healey L, Krentzel AA, Macedo-Lima M, Vahaba D. Species diversity matters in biological research. *Policy Insights Behav Brain Sci* 4: 210–218, 2017. doi:10.1177/2372732217719908.

Salgado S, Kaplitt MG. The nucleus accumbens: a comprehensive review. *Stereotact Funct Neurosurg* 93: 75–93, 2015. doi:10.1159/000368279.

Satta R, Certa B, He D, Lasek AW. Estrogen receptor betain the nucleus accumbens regulates the rewarding properties of cocaine in female mice. *Int J Neuropsychopharmacol* 21: 382–392, 2018. doi:10.1093/ijnp/pyx118.

Sazdanovic M, Slobodanka M, Zivanovic-Macuzic I, Jeremic D, Tanaskovic I, Milosavljevic Z, Malikovic A, Ognjanovic N, Sazdanovic P, Jovanovic B, Jovanovic J, Todorovic M, Toseveski J. Sexual dimorphism

of medium-sized neurons with spines in human nucleus accumbens. *Arch Biol Sci* 65: 1149–1155, 2013. doi:10.2298/ABS1303149S.

Schier CJ, Marks WD, Paris JJ, Barbour AJ, McLane VD, Maragos WF, McQuiston AR, Knapp PE, Hauser KF. Selective vulnerability of striatal D2 versus d1 dopamine receptor-expressing medium spiny neurons in HIV-1 tat transgenic male mice. *J Neurosci* 37: 5758–5769, 2017. doi:10.1523/JNEUROSCI.0622-17.2017.

Sebel LE, Graves SM, Chan CS, Surmeier DJ. Haloperidol selectively remodels striatal indirect pathway circuits. *Neuropsychopharmacology* 42: 963–973, 2017. doi:10.1038/npp.2016.173.

Shansky RM, Woolley CS. Considering sex as a biological variable will be valuable for neuroscience research. *J Neurosci* 36: 11817–11822, 2016. doi:10.1523/JNEUROSCI.1390-16.2016.

Sherborne AL, Thom MD, Paterson S, Jury F, Ollier WE, Stockley P, Beynon RJ, Hurst JL. The genetic basis of inbreeding avoidance in house mice. *Curr Biol* 17: 2061–2066, 2007. doi:10.1016/j.cub.2007.10.041.

Shuen JA, Chen M, Gloss B, Calakos N. Drd1a-tdTomato BAC transgenic mice for simultaneous visualization of medium spiny neurons in the direct and indirect pathways of the basal ganglia. *J Neurosci* 28: 2681–2685, 2008. doi:10.1523/JNEUROSCI.5492-07.2008.

Smith RJ, Lobo MK, Spencer S, Kalivas PW. Cocaine-induced adaptations in D1 and D2 accumbens projection neurons (a dichotomy not necessarily synonymous with direct and indirect pathways). *Curr Opin Neurobiol* 23: 546–552, 2013. doi:10.1016/j.conb.2013.01.026.

Staffend NA, Loftus CM, Meisel RL. Estradiol reduces dendritic spine density in the ventral striatum of female Syrian hamsters. *Brain Struct Funct* 215: 187–194, 2011. doi:10.1007/s00429-010-0284-7.

Stanić D, Dubois S, Chua HK, Tonge B, Rinehart N, Horne MK, Boon WC. Characterization of aromatase expression in the adult male and female mouse brain. I. Coexistence with oestrogen receptors α and β, and androgen receptors. *PLoS One* 9: e90451, 2014. doi:10.1371/journal.pone.0090451.

Thibault D, Loustalot F, Fortin GM, Bourque MJ, Trudeau LE. Evaluation of D1 and D2 dopamine receptor segregation in the developing striatum using BAC transgenic mice. *PLoS One* 8: e67219, 2013. doi:10.1371/journal.pone.0067219.

Ting JT, Feng G. Recombineering strategies for developing next generation BAC transgenic tools for optogenetics and beyond. *Front Behav Neurosci* 8: 111, 2014. doi:10.3389/fnbeh.2014.00111.

Tonn Eisinger KR, Larson EB, Boulware MI, Thomas MJ, Mermelstein PG. Membrane estrogen receptor signaling impacts the reward circuitry of the female brain to influence motivated behaviors. *Steroids* 133: 53–59, 2018. doi:10.1016/j.steroids.2017.11.013.

Valjent E, Bertran-Gonzalez J, Hervé D, Fisone G, Girault JA. Looking BAC at striatal signaling: cell-specific analysis in new transgenic mice. *Trends Neurosci* 32: 538–547, 2009. doi:10.1016/j.tins.2009.06.005.

Villalon Landeros R, Morisseau C, Yoo HJ, Fu SH, Hammock BD, Trainor BC. Corncob bedding alters the effects of estrogens on aggressive behavior and reduces estrogen receptor-α expression in the brain. *Endocrinology* 153: 949–953, 2012. doi:10.1210/en.2011-1745.

Will TR, Proaño SB, Thomas AM, Kunz LM, Thompson KC, Ginnari LA, Jones CH, Lucas SC, Reavis EM, Dorris DM, Meitzen J. Problems and Progress regarding Sex Bias and Omission in Neuroscience Research. *eNeuro* 4: pii: ENEURO.0278, 2017. doi:10.1523/ENEURO.0278-17.2017.

Willett JA, Johnson AG, Vogel AR, Patisaul HB, McGraw LA, Meitzen J. Nucleus accumbens core medium spiny neuron electrophysiological properties and partner preference behavior in the adult male prairie vole, Microtus ochrogaster. *J Neurophysiol* 119: 1576–1588, 2018. doi:10.1152/jn.00737.2017.

Willett JA, Will T, Hauser CA, Dorris DM, Cao J, Meitzen J. No evidence for sex differences in the electrophysiological properties and excitatory synaptic input onto nucleus accumbens shell medium spiny neurons. *eNeuro* 3: pii: ENEURO.0147, 2016. doi:10.1523/ENEURO.0147-15.2016.

Wissman AM, May RM, Woolley CS. Ultrastructural analysis of sex differences in nucleus accumbens synaptic connectivity. *Brain Struct Funct* 217: 181–190, 2012. doi:10.1007/s00429-011-0353-6.

Wissman AM, McCollum AF, Huang GZ, Nikrodhanond AA, Woolley CS. Sex differences and effects of cocaine on excitatory synapses in the nucleus accumbens. *Neuropharmacology* 61: 217–227, 2011. doi:10.1016/j.neuropharm.2011.04.002.

Wong JE, Cao J, Dorris DM, Meitzen J. Genetic sex and the volumes of the caudate-putamen, nucleus accumbens core and shell: original data and a review. *Brain Struct Funct* 221: 4257–4267, 2016. doi:10.1007/s00429-015-1158-9.

Yager LM, Garcia AF, Wunsch AM, Ferguson SM. The ins and outs of the striatum: role in drug addiction. *Neuroscience* 301: 529–541, 2015. doi:10.1016/j.neuroscience.2015.06.033.

Yoest KE, Quigley JA, Becker JB. Rapid effects of ovarian hormones in dorsal striatum and nucleus accumbens. *Horm Behav* S0018-506X(18)30055-2, 2018. doi:10.1016/j.yhbeh.2018.04.002.

Young E, Korszun A. Sex, trauma, stress hormones and depression. *Mol Psychiatry* 15: 23–28, 2010. doi:10.1038/mp.2009.94.

Young KA, Gobrogge KL, Liu Y, Wang Z. The neurobiology of pair bonding: insights from a socially monogamous rodent. *Front Neuroendocrinol* 32: 53–69, 2011. doi:10.1016/j.yfrne.2010.07.006.

Zhang L, Warren RA. Postnatal development of excitatory postsynaptic currents in nucleus accumbens medium spiny neurons. *Neuroscience* 154: 1440–1449, 2008. doi:10.1016/j.neuroscience.2008.05.002.